The genomic basis of host and vector specificity in non-pathogenic trypanosomatids

1.1. Author names

Guy Oldrieve[1*] (0000-0003-1428-0608), Beatrice Malacart[1], Javier López-Vidal[1], Keith Matthews[1] (0000-0003-0309-9184)

1.2. Affiliation

[1.] Institute for Immunology and Infection Research, School of Biological Sciences, University of Edinburgh, Edinburgh EH9 3FL, UK

1.3. Corresponding author *

guy.oldrieve@ed.ac.uk

1.4. Keywords

Trypanosoma theileri, *Trypanosoma melophagium*, non-pathogenic, host and vector specificity

1.5. Repositories

T. melophagium DNA and RNA sequencing data, along with the draft genome assembly and its annotation, can be found under the NCBI BioProject PRJNA786535.

2. Abstract

The ability of trypanosome parasites to survive and sustain infections is dependent on diverse and intricate immune evasion mechanisms. Pathogenic trypanosomes often have broad host niches that preclude identification of host specific adaptations. In contrast, some non-pathogenic species of the genus *Trypanosoma* have highly specific hosts and vectors. *Trypanosoma theileri*, a non-pathogenic parasite of bovines, has a predicted surface protein architecture that likely aids survival in its mammalian host, distinct from the dominant variant surface glycoprotein coat of pathogenic African trypanosomes. In both species, their surface proteins are encoded by genes which account for ~10% of their genome. A non-pathogenic parasite of sheep, *Trypanosoma melophagium*, is transmitted by the sheep ked and is closely related to *T. theileri*. To explore host and vector specificity between these closely related species, we sequenced the *T. melophagium* genome and transcriptome and an annotated draft genome was assembled. *T. melophagium* was compared to 43 kinetoplastid genomes, including *T. theileri. T. melophagium* and *T. theileri* have an AT biased genome, the greatest bias of publicly available trypanosomatids. This trend may result from selection acting to decrease the genome nucleotide cost. The *T. melophagium* genome is 6.3Mb smaller than *T. theileri* and large families of proteins, characteristic of the predicted surface of *T. theileri,* were found to be absent or greatly reduced in *T. melophagium.* Instead, *T. melophagium* has modestly expanded protein families associated with the avoidance of complement-mediated lysis. The genome of *T. melophagium* contains core genes required for development, glycolysis, RNA interference, and meiotic exchange, each being shared with *T. theileri*. Comparisons between *T. melophagium* and *T. theileri*

47 provide insight into the specific adaptations of these related trypanosomatids to their

48 distinct mammalian hosts and arthropod vectors.

3. Author summary

Non-pathogenic trypanosomes can have narrow host niches, with closely related trypanosome species expanding into distinct mammalian host and insect vectors. *T. theileri*, a non-pathogenic trypanosome of bovines, is predicted to have an intricate cell surface which allows it to evade the immune response of its mammalian host. In contrast, *T. melophagium* is closely related to *T. theileri* but infects sheep and is transmitted by the sheep ked rather than tabanid flies that transmit *T. theileri*. Here, we sequence and assemble the *T. melophagium* genome to identify the genomic basis of host and vector specificity in these non-pathogenic trypanosomes. We confirm the two species are closely related, however, *T. melophagium* has a smaller genome than *T. theileri*. Most of the discrepancy in genome size is due to an expansion of putative cell surface genes in *T. theileri*. The differential investment in cell surface proteins could be due to a focus on adaptation to the mammalian host in *T. theileri* and the insect host in *T. melophagium*.

64 ## 4. Data summary

65

66 The genomes, transcriptomes and proteomes used in this study were accessed from

67 the TriTrypDB repository or NCBI. *T. theileri* genome sequencing data was

68 downloaded from NCBI SRA (SRR13482812). *T. melophagium* data generated

69 during this study is available from the NCBI BioProject PRJNA786535.

70 ## 5. Introduction

71

72 Trypanosomatidae are a family of single celled eukaryotes, characterised by a
73 specialised mitochondrial genome, the kinetoplast. Trypanosomatidae are
74 monoxenous (single host) or dixenous (two host) species. Dixenous trypanosomatids
75 are obligate parasites of a broad diversity of animals and plants whilst monoxenous
76 species are largely restricted to insects (1). However, the taxonomy of
77 trypanosomatids cannot be distilled into these two broad categories, as many
78 monoxenous species opportunistically infect vertebrates (2) and some dixenous
79 species have subsequently reverted to a monoxenous lifecycle (3).

80

81 Expansion into vertebrate hosts gave rise to clades of trypanosomatids which
82 represent medical and veterinary threats. Notably, *Trypanosoma cruzi* and
83 *Leishmania* spp. cause important diseases in humans, Chagas disease and
84 Leishmaniasis, respectively. Also, *Trypanosoma brucei* has been subjected to
85 intense molecular and cytological study as two of its subspecies, *Trypanosoma*
86 *brucei gambiense* and *Trypanosoma brucei rhodesiense*, are causative agents of
87 Human African Trypanosomiases (HAT) (4). In addition to the medical impact of
88 human African trypanosomes, other African trypanosome species such as *T. b.*
89 *brucei*, *Trypanosoma vivax* and *Trypanosoma congolense* cause morbidity and
90 mortality in livestock, constraining agricultural development (5).

91

92 Trypanosomatids diverged from other eukaryotes over a billion years ago (6, 7) and
93 possess unique adaptations at the genome level (8). The *T. brucei* genome
94 comprises 11 megabase chromosomes (9) along with ~5 intermediate chromosomes

95 and ~100 mini-chromosomes (10, 11). Nuclear DNA is highly compact, and genes
96 are organised into polycistronic units, the primary transcripts of which are trans-
97 spliced and polyadenylated to resolve mature mRNA (12, 13). Their distinct
98 mitochondrial genome, the kinetoplast, consists of mini (14, 15) and maxicircles (16,
99 17) that rely upon RNA editing to generate functional mRNA (8).
100
101 The divergence in trypanosomatid morphology, transmission, and lifecycle
102 development has facilitated an adaption to a diverse range of hosts and vectors. The
103 different surface protein environments of *T. brucei*, *T. cruzi* and *Leishmania* spp.
104 exemplify the variant strategies adopted by these parasites to evade the immune
105 systems of their hosts and vectors. For example, *T. brucei* is extracellular and
106 proliferates in the blood and tissue of mammals. Its cell surface is encoded by a very
107 extensive repertoire of variant surface glycoproteins (VSGs) (10, 18). VSG variation
108 is essential to sustain long-term infections, during which antigenically distinct VSG
109 protein types dominate at each peak, facilitating host immune evasion (19, 20). *T.*
110 *cruzi* is an intracellular parasite of wild and domestic mammals. The nuclear genome
111 contains an expanded family of mucin genes that represent up to 6% of the genome
112 (21) and, along with trans-sialidases (22), these genes enable sustained infections.
113 *Leishmania* spp. are intracellular trypanosomatids whose cell surface is covered by a
114 thick layer of glycoconjugates, including families of major surface proteases (MSPs)
115 (23).
116
117 Studies have largely focused on pathogenic dixenous trypanosomatids, which can
118 hold broad host niches, capable of infecting multiple mammalian species (24). In
119 contrast, non-pathogenic dixenous trypanosomes can be highly specific to their host

120 and vector. These species represent an attractive model to study the basis of host
121 and vector specificity.
122
123 *Trypanosoma theileri* is a non-pathogenic bovine parasite which has a reported
124 prevalence of 80% in cattle in the US and Europe when screened via culture-based
125 methods (25-28). *T. theileri* is transmitted by tabanid flies (29). It can cause lifelong
126 infections but remains at an extremely low parasitaemia in immunocompetent
127 animals, indicating the presence of an effective host immune evasion mechanism or
128 strict self-imposed population control, which prevents overt disease (30, 31).
129 Experimentally, *T. theileri* can sustain an infection for at least 12 weeks (28) which,
130 combined with their non-pathogenic nature, has stimulated development of *T. theileri*
131 as a potential vaccine delivery vehicle (28). The genome of *T. theileri* encodes five
132 predicted surface protein families. These are four unique protein families, *T. theileri*
133 putative surface proteins (TTPSPs) and one MSP family (32). Together these genes
134 represent 9% of the genome of *T. theileri*, comparable to the representation of the
135 VSG gene family in *T. brucei.* Lastly, the trans-sialidases that characterise *T. cruzi*
136 were also found to be highly expressed in *T. theileri*. These findings led to the
137 suggestion of a novel immune evasion mechanism in *T. theileri,* contrasting with the
138 well-known system in African trypanosomes and distinct from that in *T. cruzi* or
139 *Leishmania* (32).
140
141 *Trypanosoma melophagium* is another non-pathogenic trypanosome of the
142 subgenus *megatrypanum*, transmitted between sheep via the sheep ked. This
143 flightless insect vector has been eradicated from much of its original geographic
144 distribution due to widespread pesticide use. However, where the sheep ked

145 persists, it often carries *T. melophagium* (33, 34). In a study of organic sheep farms,
146 *T. melophagium* was found to be present in 86% of keds, however, blood smears
147 from sheep on the same farms did not detect trypanosomes (34). Other surveys via
148 blood culture found 7.8% of sheep to be infected with *T. melophagium* (35). It has
149 historically been argued that *T. melophagium* is a monoxenous parasite of the sheep
150 ked and that the mammalian host is obsolete for transmission (36-38). However,
151 extensive studies demonstrated a mammalian host is required (39). Experimental
152 infections of sheep with *T. melophagium* suggested the longest infection lasts three
153 months and there is no lasting immunity as sheep can be reinfected with *T.*
154 *melophagium* after several months of isolation (33, 39, 40)

155

156 Molecular markers place *T. melophagium* as a close relative to *T. theileri* (34). SSU
157 rRNA is ~98% similar between *T. theileri* and *T. melophagium* isolates (33).
158 Presumably the divergence of *T. theileri* and *T. melophagium* is associated with their
159 discrete host niches (33, 34). Nonetheless, *T. theileri* and *T. melophagium* undergo a
160 similar transmission cycle where metacyclic forms are produced in the insect hindgut
161 and the infective forms are then believed to be transmitted to their mammalian host
162 via the mouth, by ingestion of insect faeces or the whole insect body. Trypanosomes
163 then invade their mammalian hosts and proliferate in the blood, before being taken
164 up as a bloodmeal by their insect vector (29, 39).

165

166 A notable contrast in the biology of these parasites is the divergence in the life
167 history of their vectors. Sheep keds, which transmit *T. melophagium*, spend their
168 entire life attached to either the skin or wool and hair of sheep. Both male and female

169 keds feed on their mammalian host (41). Tabanids, which transmit *T. theileri*, breed
170 and lay their eggs in soil, water, or trees. The larvae and pupae stages live on
171 vegetation and soil. Only female adults feed on mammalian blood, which is essential
172 for egg production. Although adult tabanids show considerable adaptation to blood
173 feeding, they also feed on the sugars of plants (42).
174
175 Here we derive the *T. melophagium* genome and compare its features with *T. theileri*
176 to provide insight into the biological specificity exhibited by each parasite in the
177 context of their close phylogenetic relationship.

178 ## 6.1. Methods

179

180 **Trypanosome culture, DNA/RNA extraction and sequencing**

181 *T. melophagium* was isolated from sheep blood collected on the island of St Kilda,
182 Scotland (Kindly provided by Professor Josephine Pemberton, University of
183 Edinburgh). Whole blood was collected into heparinized vacutainers and used within
184 2 days. 1 ml of blood was diluted with 5 volumes of a 50% mix of HMI9
185 supplemented with 20% FBS and MDBK conditioned medium. All cultures were kept
186 at 37°C and were examined microscopically every 3 days for 6 weeks. After
187 propagation of *T. melophagium* by culturing of the blood sample, the specimens
188 were transferred and co-cultured with fibroblast-like primary cells as feeder cells,
189 isolated from the same blood sample. Due to the short lifespan of these primary
190 cultured cells, *T. melophagium* was subsequently co-cultivated with MDBK cells and
191 then progressively adapted to axenic conditions with a 50% mix of HMI9 and MDBK
192 conditioned medium.

193

194 DNA was extracted from cultured *T. melophagium* using a MagAttract high molecular
195 weight DNA kit, following the manufacturer's instructions (Qiagen) and cleaned via
196 ethanol precipitation. The DNA was sequenced with Oxford Nanopore Technology's
197 (ONT) MinION (R9.4.1), following the Nanopore Rapid Sequencing protocol. Base-
198 calling was performed in high accuracy mode using Guppy (available at
199 https://community.nanoporetech.com/) which produced 1.059 gigabases (Gb) of
200 data. PycoQC was used to visualise the data (43). The same DNA was sequenced
201 with BGI's DNBseq (4.201Gb, 150 base pair (bp) reads). RNA was extracted with the
202 RNeasy mini kit (Qiagen) including a DNAse step, following the manufacturer's

203 instructions and sequenced with BGI's DNBseq (5.019Gb, 100bp reads). Raw DNA
204 and RNA DNBseq reads were trimmed with Trimmomatic (44).
205
206 *T. theileri* sequencing data was downloaded from NCBI. 170bp genomic
207 (SRR13482812) were used.
208
209 ***T. melophagium* genome assembly and annotation**
210 Jellyfish and GenomeScope were used to provide a k-mer based estimate of the
211 genome size and heterozygosity using the short DNA reads described above (45,
212 46).
213
214 Nanopore long reads were assembled using Wtdbg2 (47). For the polishing steps,
215 BWA-MEM (48) was used to align short reads and Minimap2 (49) was used to align
216 ONT reads. ONT reads were aligned to the Wtdbg2 draft assembly and three
217 iterations of Racon (50) followed by one round of Medaka (available at
218 https://github.com/nanoporetech/medaka) were performed. DNBseq reads were
219 mapped to the Medaka polished assembly, and two iterations of Racon were
220 performed. Short and long reads were aligned to the Racon polished assembly to
221 complete two final iterations of polishing with Pilon (51). At each stage of polishing,
222 the draft genome was assessed using scaffold_stats.pl (available at
223 https://github.com/sujaikumar/assemblage) and BUSCO (52).
224
225 Both sets of reads were mapped to the draft assembly. Each contig was subjected to
226 a DIAMOND blastx search against the InterProScan database (53, 54). The resulting
227 alignments and DIAMOND hits were visualised with BlobTools (55). Two contigs

228 were outliers in comparison to the rest of the assembly at under 100x coverage and
229 consisting of only 3,975 and 1,892 base pairs (Fig. S2a). These contigs were
230 removed from the assembly. BUSCO and BlobTools were re-run on this trimmed
231 assembly to assess the final assembly's completeness and coverage
232 (Supplementary Fig. S2b).
233
234 Repeat sequences in the genome were identified and soft-masked using
235 RepeatModeler2 and RepeatMasker (56). BRAKER2 was used to annotate the soft-
236 masked genome in ETP mode. The OrthoDB v10 protozoa database was utilised for
237 protein hints (57) with the addition of the *T. theileri* proteome and RNAseq evidence
238 (53, 58-68). BRAKER2 produced the protein and transcript files utilised in the
239 following analysis. The *T. melophagium* proteome was functionally annotated using
240 InterProScan (54) using the Pfam and SignalP databases (69, 70). Genome
241 conservation of collinearity was compared using D-Genies (71).
242
243 Publicly available genomes, transcriptomes and proteomes were accessed from
244 TriTrypDB (72) along with the *Phytomonas* EM1 assembly which was accessed from
245 NCBI (73). The quality of the proteomes were assessed using BUSCO; only isolates
246 which had > 85% complete proteomes were included, which left 43 isolates along
247 with *T. melophagium*. A list of all the isolates used in this study can be found in the
248 Supplementary File S1. The assembly statistics of the 44 genomes were assessed
249 using scaffold_stats (available at https://github.com/sujaikumar/assemblage).
250
251 The genomes from each of these trypanosomatid isolates were screened for transfer
252 RNA genes using tRNAscan-SE (74). The outputs of these results were used to infer

253 the strength of selection acting on translational efficiency and nucleotide cost for
254 each isolate, along with the background mutation bias, using CodonMuSe (75, 76).
255 Each isolate was assessed using 1) every CDS, 2) single copy universal orthologs
256 (identified in the orthologous protein clustering steps below) (n=992) and 3) single
257 copy universal orthologs which are essential for every stage of the *T. brucei* life cycle
258 (n=158). The last list of genes were identified by screening the universal single copy
259 orthologs for genes which had a significant reduction in transcript levels in every
260 library of an RNAi phenotype screen (>1.5 log fold decrease) (77).
261
262 **Orthology inference**
263 Orthologous proteins from 44 trypanosomatid proteomes were identified with
264 OrthoFinder (78) and protein clusters were summarised with KinFin (79), using
265 InterProScan annotations based on the Pfam and signalP databases (54, 69, 70). A
266 minimal cut-off threshold was not applied to the orthogroup annotation. The
267 orthogroup annotation summary can be found in Supplementary File S2. A species
268 tree was produced by STAG and STRIDE, as part of the OrthoFinder analysis (80,
269 81) which was visualised with iTOL (82). STRIDE identified *Bodo saltans* as the best
270 root for the consensus species tree.
271
272 To confirm the absence of VSGs in *T. melophagium*, all CDS sequences labelled as
273 'VSG' in the *T. brucei* TREU927/4 reference genome were downloaded from
274 TriTrypDB. A blastn search was performed with the *T. melophagium* genome as the
275 database using a loose cut-off (e-value = 1e-5). A similar search was performed to
276 confirm the reduced TTPSP counts in *T. melophagium*. For this, the *T. theileri*

277 transcripts were used to query a database made from the *T. melophagium*

278 transcripts (e-value = 1e-25).

279

280 The cell surface orthogroups in this study were annotated with the orthogroups from

281 Kelly *et al*. 2017 (32) based on the orthogroup membership of genes in the two

282 analyses. Unless stated otherwise, all of the figures in this study were plotted in R

283 (83) using ggplot2 (84) and ggrepel (85).

284

285 The full list of tools used in this study, and the options used to run those tools, can

286 be found in Table S1.

287 ## 6.2. Results

288

289 ***T. melophagium* genome assembly**

290 An initial assessment of the *T. melophagium* genome, via k-mer counting, predicted
291 that it was smaller than that of *T. theileri* (22.3 Mb and 27.6 Mb, respectively), this
292 variation being observed in its repeat and unique sequence (Table 1). Notably, both
293 genomes are predicted to have extremely low heterozygosity (0.30 and 0.41 for *T.*
294 *melophagium* and *T. theileri,* respectively) in comparison to other *Trypanosoma*
295 isolates (86). Large gene families, such as the TTPSPs, only account for ~10% of
296 the *T. theileri* genome and so are predicted to have a minor effect in the
297 heterozygosity calculation. The k-mer counting prediction was similar in size to the
298 final assembly (Table 1). The *T. melophagium* assembly consisted of 64 contigs in
299 comparison to 253 for *T. theileri*. BUSCO assessments suggest both assemblies are
300 100% complete, although *T. theileri* is slightly fragmented (Table 1).

301 **Table 1:** Genome assessment. The assemblies used in this assessment represent
302 the final draft of the *T. melophagium* assembly produced during this study and the *T.*
303 *theileri* assembly available from TriTrypDB (32, 72). The k-mer spectra plots
304 associated with the first section of the table are found in Fig. S1.

	T. melophagium	***T. theileri*** (32)
k-mer based genome survey		
Heterozygosity (%)	0.30	0.41
Genome / repeat / unique length (Mbp)	22.28 / 4.16 / 18.13	27.62 / 7.97 / 19.65
Genome assembly statistics (for scaffolds longer than 200 bp)		
Number of contigs	64	253
Span (Mbp)	23.3	29.6
Min / Max / Mean (bp)	5,186 / 1,230,212 / 364,120	791 / 1,635,300 / 117,005
N50	505,851	517,122
GC (%)	41.2	40.1
Genome BUSCO assessment		
Complete/ Single copy/ Duplicated/ Fragmented	100 / 100 / 0 / 0	99.2 / 99.2 / 0 / 0.8
Annotation		
Number of genes	10,057	11,312
Annotation BUSCO assessment		

Complete/ Single copy/ Duplicated/ Fragmented	100 / 100 / 0 / 0	99.2 / 99.2 / 0 / 0.8

305

306 The *T. melophagium* and *T. theileri* genomes were aligned to highlight the
307 conservation of collinearity. The conservation is more similar to the conservation
308 between the species *T. brucei* TREU927/4 *and T. congolense* IL3000 2019 than
309 between isolates of the same species, *T. brucei* TREU927/4 and *T. brucei* Lister 427
310 (Fig. 1 & Fig. S3). The *T. melophagium* genome was annotated with 10,057 proteins,
311 in comparison to 11,312 in *T. theileri* (Fig. 2c & Table 1) (32).
312
313 Trypanosomatid genomes, proteomes and transcriptomes were downloaded from
314 TriTrypDB (72). Proteome completeness was assessed with BUSCO. Those above
315 85% complete were retained, leaving 44 isolates from 9 genus (Supplementary File
316 S1). *T. theileri* and *T. melophagium* have some of the smallest genomes in this study
317 group and have the lowest GC content (40.1% and 41.2%, respectively), contrasting
318 with the trypanosomatid mean of 48.4% (Fig. 2a).
319
320 Environmental temperature, generation time, neutral drift, gene splicing, tRNAs,
321 translational accuracy/efficiency and protein folding have all been hypothesised to
322 cause codon bias. However, codon bias can be influenced by nutrient availability
323 (76). Species with low nitrogen availability, such as the plant trypanosomatid,
324 *Phytomonas*, have an AT rich genome, potentially to mitigate the lack of nitrogen in
325 their plant hosts (76). Selection acting on genome nucleotide cost (Sc) is in
326 competition with selection acting to alter the translational efficiency of the genome
327 (St) (75, 76). Based on universal single copy orthologues, selection pressure acting
328 on the translational efficiency is minimal for both *T. theileri* and *T. melophagium*. In
329 contrast, they show the greatest predicted selection pressure acting to reduce the
330 nucleotide cost of any trypanosomatid genome. The AT biased content can be

331 interpreted as a remodelling of the *T. theileri* and *T. melophagium* genomes to
332 reduce the cost of the genome (Fig. 2 a & b). This pattern held true when every CDS
333 was compared (Fig. S4 a & b) and in universal single copy orthologs which are
334 essential for every life cycle stage of *T. brucei* (Fig. S4 c & d).

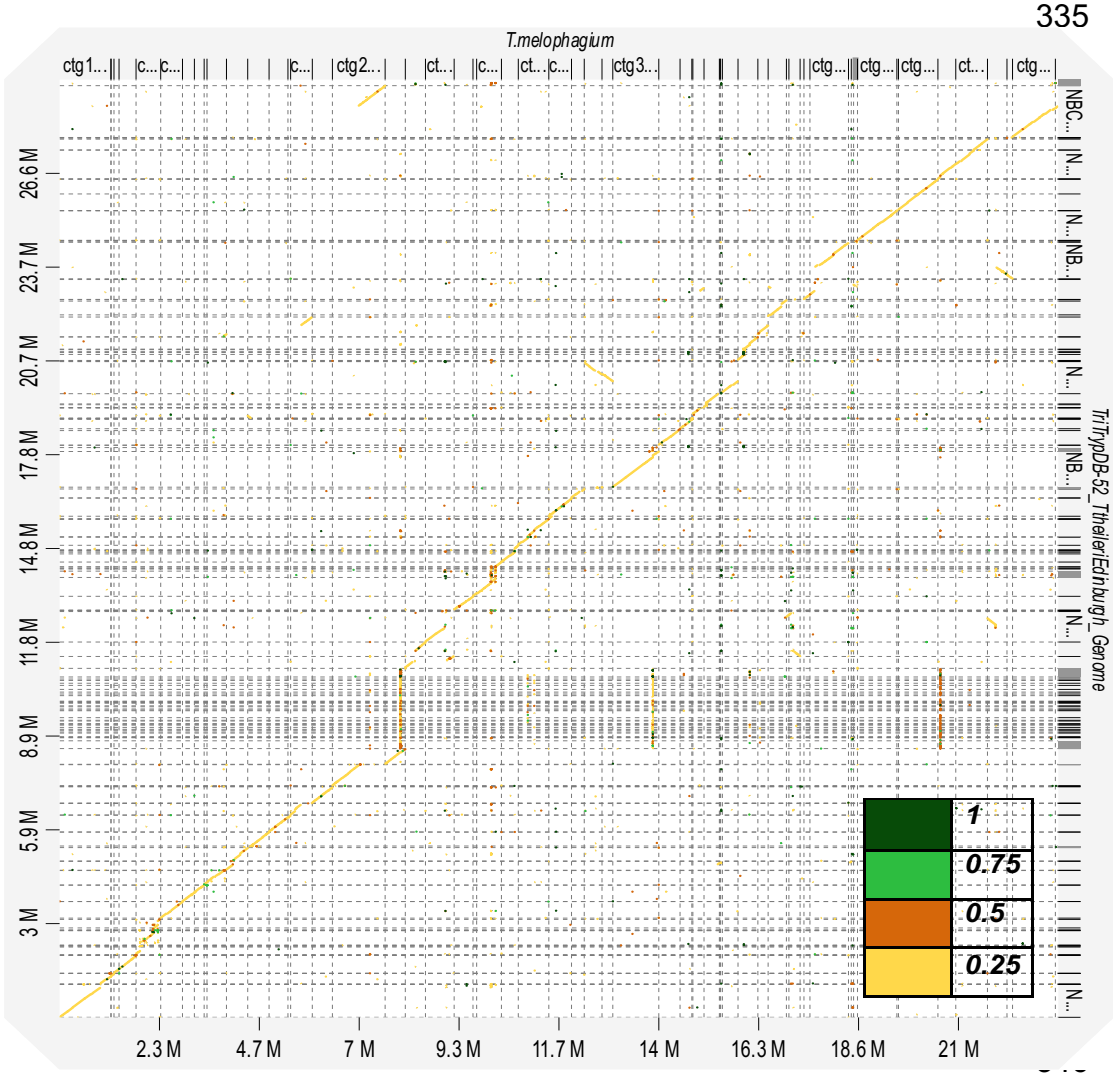

Figure 1: Synteny of the *T. melophagium* and *T. theileri* genome sequences highlights conservation and identity between the two species. The legend refers to the percentage identity between the sequences.

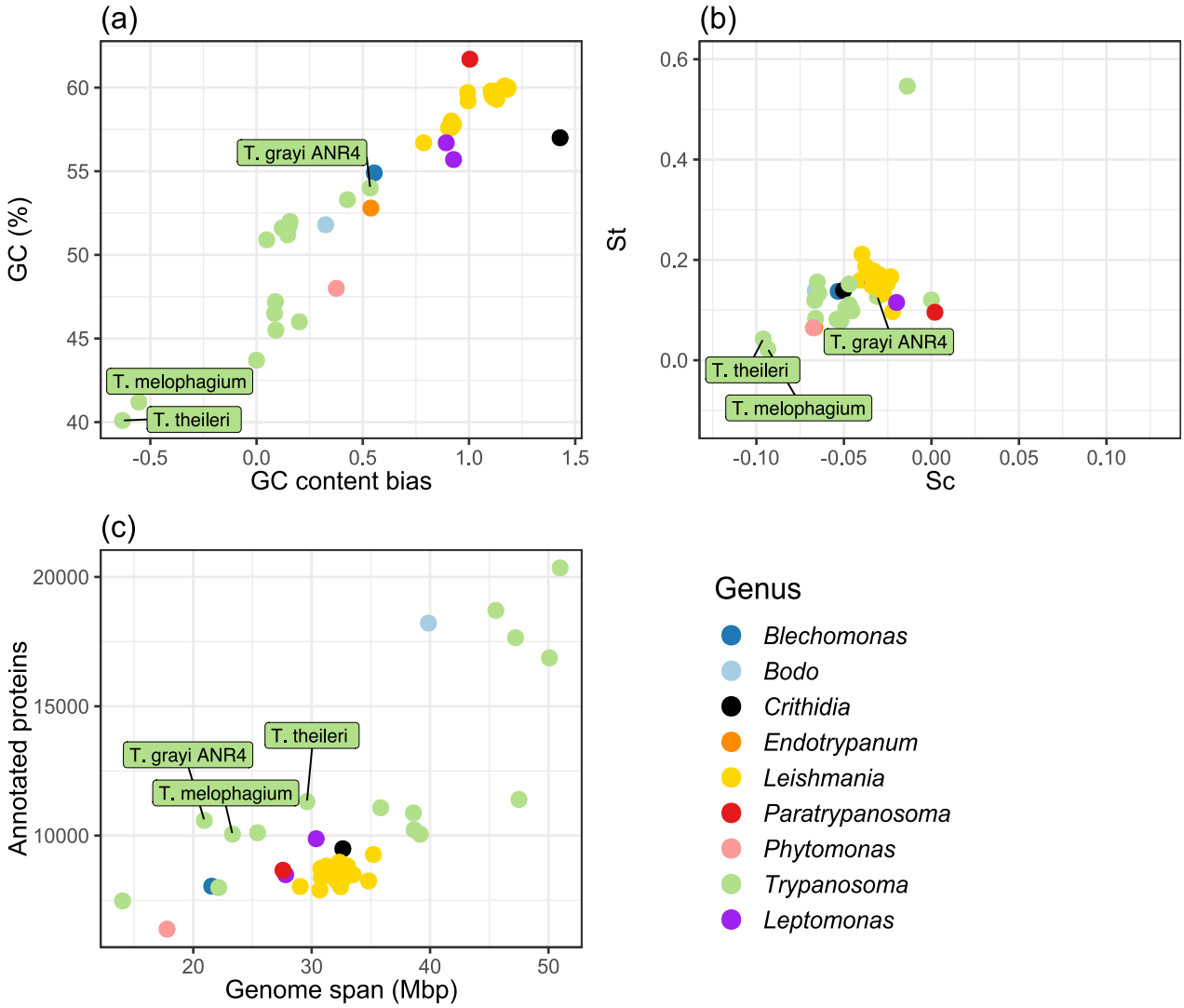

350

351 **Figure 2:** (a) GC content across the whole genome and GC content bias in the CDS
352 of trypanosomatid universal single copy orthologues (n=992). GC content (GC) > 0 =
353 GC content bias. GC < 0 = AT content bias. (b) Selection acting on translational
354 efficiency (St) and selection acting on nucleotide cost (Sc) in trypanosomatid
355 universal single copy orthologues. Sc > 0 = Selection acting to increase codon
356 nucleotide cost. Sc < 0 = Selection is acting to decrease codon nucleotide cost. St >
357 0 = Selection is acting to increase codon translational efficiency. St < 0 = Selection
358 acting to decrease codon translational efficiency. (c) Counts of annotated protein
359 sequences of publicly available trypanosomatids compared by genome size.

360 **Orthologous protein clustering and phylogenetic inference**

361 Orthologous clustering identified genes that descended from a gene in the last
362 common ancestor of the 44 trypanosomatid proteomes used in this study (Fig. 2,
363 Supplementary File S1). From the 44 proteomes, 18,274 orthogroups were identified
364 (96.5% of the proteins used in this study were included in one of these orthogroups),
365 992 orthogroups were single copy and contained all isolates.

366

367 A species tree was generated as part of the orthologous protein clustering. Using
368 genetic markers, previous studies have noted the similarity between *T. melophagium*
369 and *T. theileri* (33, 34). Based on 2,312 gene trees, *T. theileri* is the closest isolate to
370 *T. melophagium* and groups with the stercorarian trypanosomes, which include *T.*
371 *cruzi*, *Trypanosoma grayi* and *Trypanosoma rangeli,* rather than with salivarian
372 trypanosomes such as *T. brucei* (Fig. 3). *T. grayi* is the closest isolate to the *T.*
373 *melophagium* and *T. theileri* clade and is closer in size to the genome span of *T.*
374 *melophagium* than to *T. theileri* (Fig. 2c). *T. melophagium* and *T. theileri* do seem to
375 be closely related species with relatively short branch lengths (0.093 and 0.088
376 substitutions per site, respectively). In comparison, *T. congolense* is more divergent
377 from *T. brucei* (0.249) whilst the isolates within *T. brucei* (*T. brucei brucei* Lister
378 427:0.0009, *T. brucei evansi* STIB805: 0.003, *T. brucei brucei* TREU927/4: 0.003
379 and *T. brucei gambiense* DAL972:0.004) show less divergence than seen between
380 *T. theileri* and *T. melophagium*.

381

382 *T. theileri* has a greater number of species-specific orthogroups than *T.*
383 *melophagium* and 12.9% of its genes are assigned to one of these orthogroups,
384 while *T. melophagium* has only 2.7% of its genes in a species specific orthogroup

385 (Table 2). Terminal branch length is correlated with specific orthogroup counts,
386 which could account for the discrepancy. However, *T. melophagium* and *T. theileri*
387 are each other's most recent common ancestor and have been evolving at a roughly
388 similar rate since this time, with similar terminal branch lengths (Fig. 3). To visualise
389 these differences, the number of genes in each orthogroup was compared between
390 *T. melophagium* and *T. theileri*. Orthogroups associated with host interaction protein
391 families were highlighted based on their identification as a putative cell surface
392 protein by Kelly *et al*. 2017 (32). Many of the *T. theileri* species specific orthogroups
393 expansions belong to a cell surface family (Fig. 4a).

394 **Table 2:** Orthologous protein clustering statistics of *T. melophagium* and *T. theileri*.

395 The full species-specific clustering summary can be found in Supplementary File S3.

	T. melophagium	*T. theileri*
Number of genes	10,057	11,312
Genes in orthogroups (%)	97.3	97.4
Orthogroups containing species (%)	43.9	44.2
Number of species-specific orthogroups	76	121
Genes in species-specific orthogroups (%)	2.7	12.9
Comparatively expanded orthogroups	787	563

396

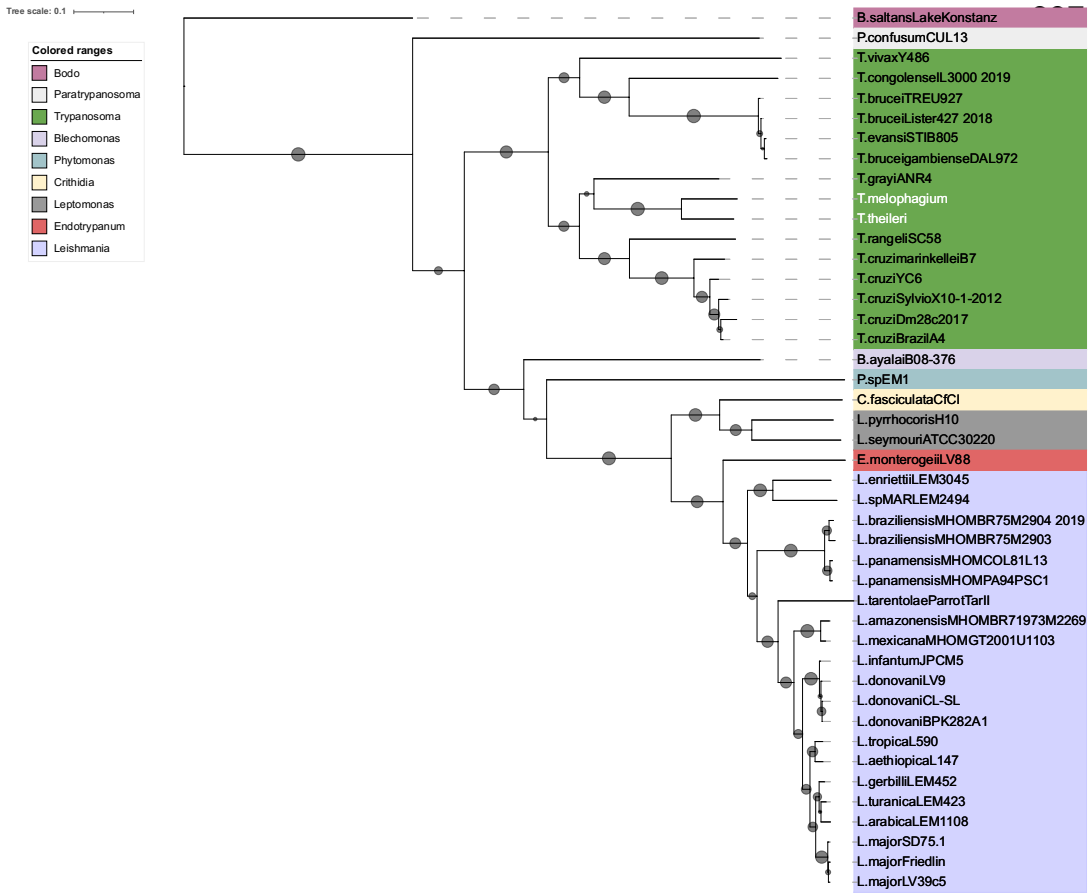

Figure 3: Species consensus tree based on 2,312 species trees created by STAG and STRIDE, OrthoFinder. The support values are represented by circles. Support values correlate to the proportion of times that the bipartition is seen in each of the individual trees used to create the consensus tree. The scale represents substitutions per site.

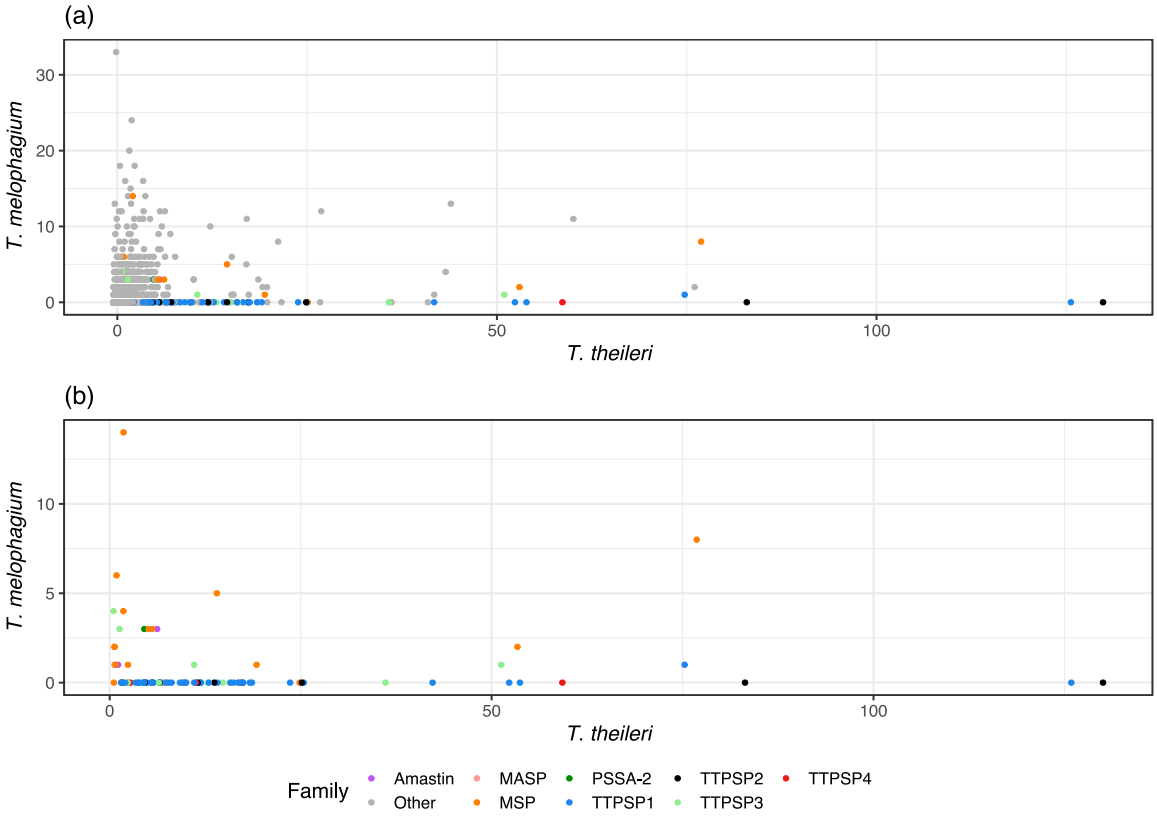

Figure 4: (a) Orthogroup and (b) host interaction orthogroup size comparison between *T. melophagium* and *T. theileri*. Each dot represents the numbers of genes found in each orthogroup for both species. The orthogroups have been annotated with their designation as either a putative cell surface protein family or 'other' (32).

409 **Interaction with the mammalian host and predicted cell surface proteins**

410 Firstly, and as expected, *T. melophagium* was found to lack any genes in
411 orthogroups which contained VSGs, characteristic of African trypanosomes
412 (Supplementary File S4). To validate this, a blast search was performed using a
413 relaxed cut off (1e-5) using the *T. melophagium* genome as the database and *T.*
414 *brucei* TREU927/4 VSGs as the query. No hits were identified.

415

416 To enable comparison to the *T. theileri* genome analysis, the genes and orthogroups
417 from this study were annotated with orthogroups from Kelly *et al*. (2017) (32). Across
418 the entire genome, *T. theileri* is predicted to contain 1,265 more genes than *T.*
419 *melophagium* (Table 1). Examination of orthogroups which were associated with a *T.*
420 *theileri* putative surface protein (TTPSP) revealed a large expansion in *T. theileri*
421 (1,251 genes) compared to *T. melophagium* (10 genes) which could equate to much
422 of the disparity in genome size (Fig. 4). To confirm the difference in TTPSPs, the *T.*
423 *theileri* transcripts were subjected to a blastn search against a database consisting of
424 the *T. melophagium* transcripts (1e-25 cut-off). The *T. melophagium* transcripts were
425 derived from the genome annotation analysis. Only 9 *T. theileri* TTPSPs aligned to *T.*
426 *melophagium*.

427

428 TTPSPs were split between four orthogroups in the original *T. theileri* genome
429 analysis but were split between 66 orthogroups in this analysis (Table 3) (32).
430 TTPSPs share conserved C terminal GPI addition and N terminal signal sequences
431 and contain regions of high divergence in the remainder of the sequence. TTPSPs
432 are highly expressed as a family at the population level and are largely contained
433 within tandem arrays, highlighting a similarity to the VSGs of *T. brucei* (32).

434 Excluding *T. melophagium*, TTPSPs are absent from all other kinetoplastid species
435 analysed (Supplementary File S4) revealing their specific innovation in these related
436 trypanosomatids.
437
438 Following the TTPSPs, the largest expanded gene family in *T. theileri* are the MSPs.
439 This protein family belongs to the peptidase M8 family of metalloproteinases. MSPs
440 are likely to have contrasting roles in different life stages but their best understood
441 function is to bind and cleave members of the complement system. This role
442 presumably allows for evasion of complement-mediated proteolysis and therefore
443 assists survival in the insect and mammalian hosts (23). Orthogroups which
444 annotated as MSPs were expanded in *T. melophagium*, such as OG0008865. *T.*
445 *melophagium* also has a species specific orthogroup (OG0009903) consisting of 11
446 proteins and annotated as leishmanolysin, indicative of cell surface protein families.
447 Combined, these results suggest that the surface protein environment of *T.*
448 *melophagium* and *T. theileri* are distinct and that genes encoding these proteins
449 account for most of the discrepancy in the genome sizes.

450 **Table 3:** Cell surface orthogroup counts from Kelly *et al*. (2017) (32) and this study

451 along with counts of genes present in each category.

Cell surface category	Annotation	Orthogroup count Kelly *et al* / this study	Gene count *T. theileri* / *T. melophagium*
Conserved	Amastin	1 / 2	7 / 4
Conserved	MASP	1 / 1	1 / 1
Conserved	MSP	1 / 18	229 / 52
Conserved	PSSA-2	1 / 1	5 / 3
Unique	TTPSP1	1 / 42	720 / 1
Unique	TTPSP2	1 / 10	301 / 0
Unique	TTPSP3	1 / 11	157 / 9
Unique	TTPSP4	1 / 3	73 / 0

452

453 **Clade and species specific orthogroups**

454 *T. grayi*, *T. melophagium* and *T. theileri* contain 42 clade-specific orthogroups
455 including the MSP orthogroups OG0000590 and OG0008095. Both orthogroups
456 were expanded in *T. theileri* in comparison to *T. grayi* and *T. melophagium*. *T.*
457 *melophagium* and *T. theileri* share 81 orthogroups specific to the two species.
458 Twelve of the orthogroups are putative cell surface protein families, including five
459 representatives from TTPSP and seven MSP orthogroups. Of the nine-remaining
460 annotated orthogroups, OG0008096 is the largest and contains trans-sialidsases.
461 The orthogroup is expanded in *T. theileri* (n=17) compared to *T. melophagium* (n=5).
462

463 *T. theileri* has 121 species specific orthogroups. Sixty-four of these were putative
464 host interaction genes (32). Two annotated orthogroups remained, which included a
465 leucine rich repeat family associated with protein binding and (OG0011868) and a
466 calpain cysteine protease family (OG0018204). *T. melophagium* has 76 species
467 specific orthogroups, 68 of these were unannotated. Leishmanolysin families were
468 annotated in three of the remaining orthogroups (OG0009903, OG0013746 and
469 OG0013747). This annotation is associated with cell adhesion, such as MSP
470 families. Other annotated species-specific orthogroups consisted of an actin family
471 (OG0018163) along with several families associated with protein binding, WD
472 domain G-beta repeat (OG0018131) and a leucine rich repeat family (OG0018098).

473 **Modifying enzymes**

474 Trans-sialidases are differentially expanded in *T. theileri* and *T. melophagium*, with
475 38 and 8 genes, respectively. Of the four orthogroups containing trans-sialidase, two
476 do not contain proteins from *T. melophagium* (OG0011818 and OG0015016). These
477 two orthogroups contain proteins from *T. cruzi* and so are likely to have been lost by
478 *T. melophagium* and *T. grayi.* In *T. cruzi*, trans-sialidases are involved in host
479 immune evasion (22).

480

481 Invertases are typical of the cell surface of *Leishmania* and is thought to transform
482 sucrose into hexose in the gut of the vector. The orthogroups (OG0000150 and
483 OG0000409) that include 20 *T. theileri* invertase genes only have 3 members in *T.*
484 *melophagium* and 3 members in *T. grayi*. This expansion might indicate an
485 adaptation of *T. theileri* to its vector, the tabanid fly, which can feed on sugary flower
486 nectar (87). In contrast, the *T. melophagium* vector, the sheep ked, exclusively feeds
487 on mammalian blood. The orthogroups with *T. theileri* invertases contain only one
488 gene from the plant parasite *Phytomonas* (88, 89), suggesting a different mechanism
489 for sucrose metabolism in these parasites.

490

491 Other putative cell surface modifying molecules, such as UDP-galactose/UDP-N-
492 acetylglucosamine transferases (OG0000001) were expanded in *T. theileri* (n=60)
493 compared to *T. melophagium* (n=11).

494 **Glycolysis**

495 Transcriptome comparison between *T. brucei* and *T. theileri* revealed differences in
496 abundance of glycosomal enzyme mRNAs. Particularly, pyruvate orthophosphate
497 dikinase, phosphoenolpyruvate carboxykinase and malate dehydrogenase were
498 found to be >10 fold more abundant in *T. theileri* than in *T. brucei* (32). When
499 comparing glycolysis-related genes in *T. melophagium* and *T. theileri*, we found that
500 *T. melophagium* has expanded the number of genes in three of the orthogroups
501 associated with glycolytic enzymes. These included pyruvate orthophosphate
502 dikinase (OG0000570), phosphoenolpyruvate carboxykinase (OG0000120) and
503 malate dehydrogenase (OG0000332), whilst *T. melophagium* has a reduced
504 numbers of genes in the fumarate reductase orthogroup (OG0000078). Orthogroups
505 associated with peroxisome targeting were found to be in equal numbers
506 (OG0004108 PEX5 and OG0003998 – PEX7). All other glycolysis-related genes
507 included in the comparison are present in equal numbers in the two species.
508 Therefore, it is likely that the glycolysis pathway is conserved in *T. melophagium.*

509 **Life cycle**

510 Extensive studies of *T. brucei* have identified genes which are associated with key
511 stages of the *T. brucei* life cycle. These studies tracked genes associated with
512 stumpy formation in the blood stream form (90-93) and regulators of
513 metacyclogenesis (94). These genes were combined with a list of validated
514 development associated genes such as the RNA binding proteins RBP6, RBP7,
515 RBP10 and ZFP2 and ZFP3 along with developmental regulators NRK A, NRK B,
516 RDK1, RDK2, MAPK2 and phosphatases such as PTP1 and PIP39 (95-102). Most
517 of the orthogroups containing these genes were represented with a similar number of
518 genes in each species, indicating the presence of an environmental sensing ability
519 and developmental competence (Fig. 5). However, there were notable differences.
520 There is an expansion in the orthogroups containing KRIPP14, which is a
521 mitochondrial SSU component (90), in *T. theileri*. *T. melophagium* has expanded its
522 orthogroups containing the kinases NRK (96, 100), NEK and (99) ADKF (90) along
523 with a dual specificity phosphatase (DsPho) and protein phosphatases 1 (PP1) (90,
524 103). Both *T. theileri* and *T. melophagium* are missing metacaspase (MCA1) which is
525 associated with the later stages of progression towards metacyclic forms in *T. brucei*
526 (94) and Hyp12 which upregulates bound mRNAs during development based on
527 tethering assays in *T. brucei* (90, 103). Puf11, an effector molecule required for
528 kinetoplast repositioning in epimastigotes (94), is also absent in *T. melophagium*.

529

530 Life cycle regulatory genes and genes controlling meiosis SPO11, MND1, HOP1 and
531 DMC1 were found in *T. melophagium* and *T. theileri* (Fig. 5), suggesting
532 maintenance of a sexual stage.

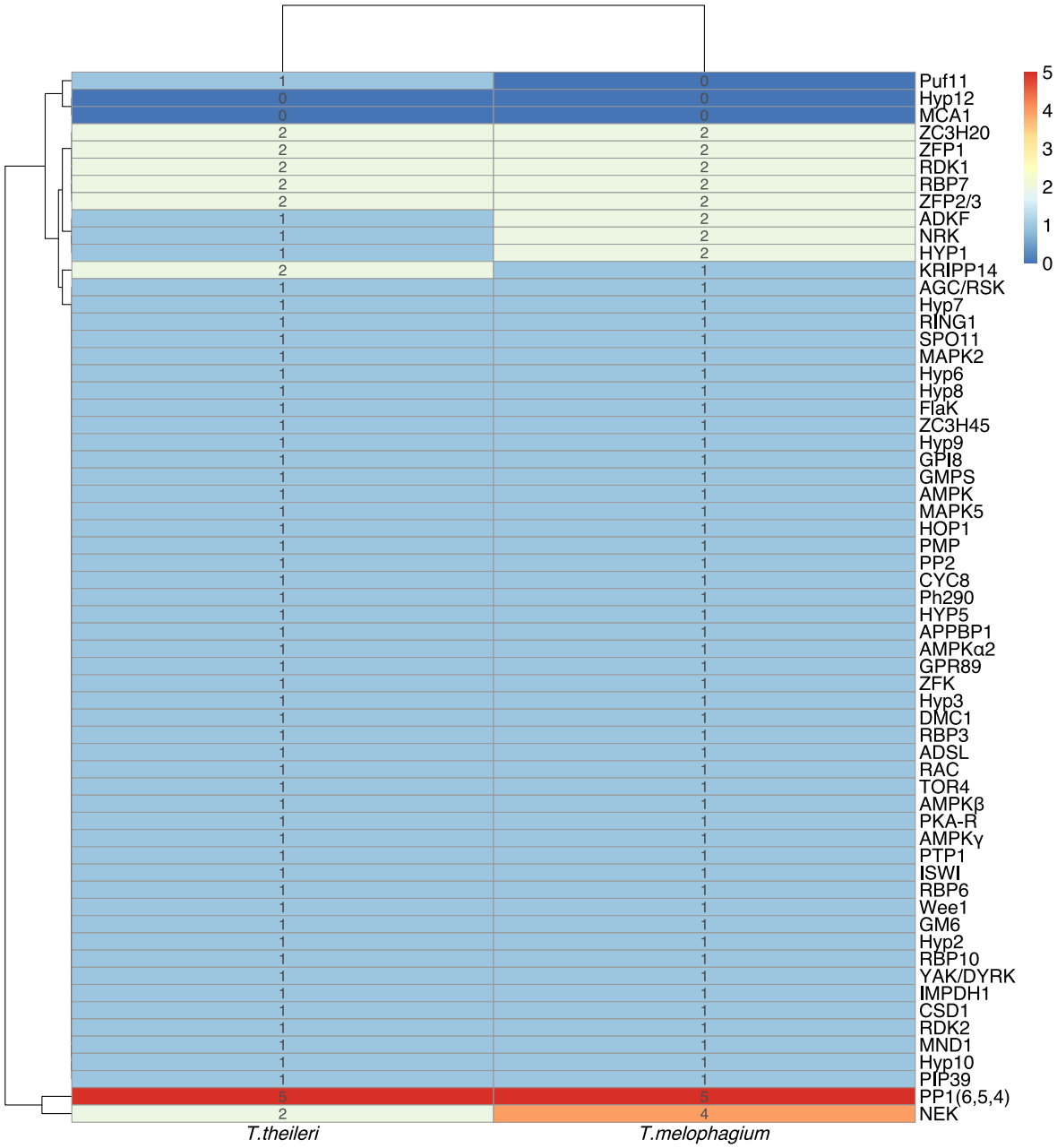

Figure 5: Genes associated with development, and related proteins, at various stages throughout the *T. brucei* life cycle. The number of genes in orthogroups associated with developmental regulation have been quantified in *T. theileri* and *T. melophagium*.

538 **RNAi**

539 All 5 core genes that represent the trypanosome RNAi machinery (AGO1, DCL1,
540 DCL2, RIF4 and RIF5) were present in *T. melophagium*, with an extra gene in the
541 orthogroup containing DLC2 (Supplementary File S4). This indicates a functional
542 gene silencing pathway is present in *T. melophagium* matching the prediction in *T.*
543 *theileri*.

544 ## 6.3. Discussion

545

546 *T. melophagium* and *T. theileri* are closely related trypanosomes that have distinct
547 hosts and vectors (33, 34). Here, the genome of *T. melophagium* was sequenced
548 and a draft assembly was produced and annotated. The annotated proteome was
549 incorporated into a comparison with *T. theileri,* and other publicly available
550 trypanosomatid proteomes, to determine their phylogenetic relationship and to
551 explore the genomic basis of the host and vector specificity of these non-pathogenic
552 trypanosomatids.

553

554 Although the two genomes compared in this analysis are predicted to be complete
555 (Table 1), their assembly and annotation were performed five years apart using
556 different pipelines and technologies. Comparing assemblies obtained using the same
557 sequencing technologies and pipelines would allow for greater confidence in the
558 observed variations in their genome content. This was not possible since many of
559 the assembly tools used are specific for the sequencing technologies whilst there
560 has been substantial development in assembly methods between the two studies.
561 However, based on the convergence of the k-mer counting based prediction with the
562 assembly sizes, along with 100% complete BUSCO scores, we were reassured by
563 the quality of the draft assemblies and the subsequent comparisons of their genome
564 content.

565

566 Using k-mer counting based predictions, *T. melophagium* was anticipated to have a
567 smaller genome than *T. theileri*. This held true when the data were assembled (Table
568 1). The *T. melophagium* genome is more similar in size to *T. grayi*, the closest

569 relative to *T. melophagium* and *T. theileri,* than to *T. theileri* (Fig. 2 & 3). *T. theileri*
570 has likely expanded its genome size since speciation occurred. A peculiarity of *T.*
571 *theileri* and *T. melophagium* is their highly reduced heterozygosity, in contrast to
572 African trypanosomes (86). It is possible this reduced heterozygosity is linked to a
573 founder effect (104). As *T. theileri* and *T. melophagium* have utilised specific host
574 and vector niches, the small population that initially expanded into the niches
575 possibly underwent a significant population bottleneck, especially as host
576 domestication caused eradication of wild progenitors and wild relatives, which could
577 have facilitated a reduction in heterozygosity, induced by genetic drift. Alternatively,
578 the absence of a sexual cycle could contribute to the reduced heterozygosity.
579 Although *T. melophagium* and *T. theileri* contain genes required for meiosis, it
580 doesn't confirm the species undergo sexual reproduction.
581
582 Selection appears to be acting to reduce the genome wide nucleotide biosynthesis
583 cost in both *T. theileri* and *T. melophagium* (Fig. 2b) which has remodelled their
584 genomes toward an AT bias, contrasting all other trypanosomatid genomes analysed
585 in this study (Fig. 2 a & c). The predicted selection pressure acting to reduce
586 nucleotide cost is at the expense of translational efficiency (Fig. 2c) and is greater
587 than the free-living *Bodo saltans*, monoxenous insect parasites such as the early
588 branching *Paratrypanosoma confusum* and *Phytomonas* EM1. *Phytomonas* has
589 limited access to nitrogen as it infects nitrogen deficient plants and has been
590 highlighted as an example where diet can cause selection to reduce the species
591 genome nucleotide cost, through a reduction in GC content (76). We propose that
592 the reduction in the selection cost of *T. theileri* and *T. melophagium* may be related

593 to their non-pathogenic nature. By remodelling their genome to an AT bias, they may
594 have reduced their cost to their host, facilitating reduced pathogenicity.
595
596 This clade specific genome remodelling provides an example of the similarity
597 between *T. theileri* and *T. melophagium*. However, the species have contrasting
598 hosts, vectors, and genome sizes. Genome annotation and orthology inference
599 identified candidates for their discrepancy in genome size. When species specific
600 orthogroups were compared, the greatest contrast was between orthogroups
601 associated with the putative cell surface, with the largest expansions detected in *T.*
602 *theileri* being of TTPSP and MSP surface protein families (Fig. 4). Although both
603 species undergo a cyclical transmission cycle, which includes mammalian and insect
604 stages, we hypothesise the respective prevalence in their mammalian hosts, and the
605 contrasting life history of their respective vectors could explain the genome
606 expansion in *T. theileri*. *T. theileri*, spread by tabanids, are found in over 80% of
607 livestock (25-28). In comparison, *T. melophagium* exhibits lower detected
608 prevalence, being rarely identified in its mammalian host via blood smears (34) or
609 after blood culture (35). Moreover, sheep keds, which transmit *T. melophagium*, are
610 intimately associated with their mammalian host, spending their entire life either on
611 the sheep's skin or wool. Here, males and females feed solely on mammalian blood
612 providing many opportunities for transmission of *T. melophagium* from the sheep to
613 the sheep ked (39). Therefore, there is potentially less advantage for *T.*
614 *melophagium* to invest in mammalian immune evasion mechanisms required to
615 extend the length of its infection in sheep, since it has many transmission
616 opportunities. The limited investment in *T. melophagium* is emphasised by their
617 relatively unsophisticated putative TTPSP repertoire alongside modestly expanded

618 species-specific MSP families (Fig. 4). Instead, *T. melophagium* could rely on its
619 ancestral ability to sustain infections in invertebrate hosts which, although able to be
620 primed to defend against a specific pathogen, rely upon an innate immune response
621 (105).
622
623 In contrast, *T. theileri* has a transient host-vector interaction. Tabanid flies of either
624 gender survive on plant sugars whilst adult females occasionally feed on mammalian
625 blood (42). Therefore, potentially *T. theileri* requires extended survival in its
626 mammalian host to sustain transmission to cattle, compared to the intimate long-
627 term association of sheep keds with *T. melophagium*. The investment from *T. theileri*
628 in an expanded surface protein repertoire is likely to support adaptive immune
629 evasion and prolonged survival in the mammalian stage of its life cycle. Alternatively,
630 or additionally, differences between the bovine and ovine immune responses could
631 contribute (106).
632
633 Many of the gene families identified in *T. theileri* (32) were further divided into
634 multiple orthogroups in this study. The discrepancy is likely to be explained by
635 evolution of the methods utilised by OrthoFinder. At the time of publication of the *T.*
636 *theileri* study, OrthoFinder v.1 was available, while our analysis used version v.2.5.
637 For this reason, we can speculate that the clustering in this study is more refined,
638 such that the TTPSP families should be divided into smaller protein families.
639 However, large paralogous orthogroups remain the toughest challenge for
640 orthogroup clustering software and so the relationships between this set of proteins
641 will continue to evolve alongside the software (107).
642

643 Genes involved in the trypanosome life cycle, cellular quiescence and meiosis were
644 all detected in *T. melophagium*, suggesting a competent developmental cycle along
645 with the machinery for sexual recombination. There is an expansion of the *T. theileri*
646 invertase orthogroup which was not present in *T. melophagium*. This is potentially
647 associated with the utilisation of sucrose in the tabanid fly's diet. Although the
648 glycolysis pathway is present in *T. melophagium*, there was an expansion in the
649 pyruvate orthophosphate dikinase, phosphoenolpyruvate carboxykinase and malate
650 dehydrogenase orthogroups. These genes are associated with the branch of the
651 glycolysis pathway that converts pyruvate to succinate to facilitate the recovery of
652 NAD^+ (32). This branch of the glycolytic pathway was upregulated in *T. theileri* in
653 contrast to *T. brucei* (32). Interestingly, the core RNAi genes were detected in *T.*
654 *melophagium*, consistent with *T. theileri* but distinct from *T. cruzi* which is also a
655 stercorarian trypanosome, but which lacks the requisite molecular machinery (108).
656
657 In summary, we have found that *T. theileri* and *T. melophagium* are closely related
658 species which display substantial remodelling of their genomes to facilitate a
659 reduction in their nucleotide costs, which could reduce the costs they impose on their
660 hosts. *T. theileri* displays a considerable genome expansion which is associated with
661 a large repertoire of unique proteins that characterise its cell surface and host
662 interaction gene repertoire. These genes could facilitate a lifelong infection in its
663 mammalian host. The comparatively unsophisticated immune evasion repertoire
664 displayed by *T. melophagium* suggests that the species has emphasised its
665 adaptation to the insect stage of its lifecycle.

7. Author statements

7.1. Authors and contributions

Guy Oldrieve (GO) 0000-0003-1428-0608

Beatrice Malacart (BM)

Javier López Vidal (JLV)

Keith Matthews (KM) 0000-0003-0309-9184

Contributor Role	Author
Conceptualisation	GO, KM
Methodology	GO, BM
Software	GO
Validation	GO
Formal Analysis	GO, BM
Investigation	GO, BM
Resources	GO, KM, JLV
Data Curation	GO
Writing – Original Draft Preparation	GO, BM
Writing – Review and Editing	GO, KM, BM, JLV
Visualisation	GO, KM, BM
Supervision	KM
Project Administration	GO, KM
Funding	KM

676 ## 7.2. Conflicts of interest

677 The authors declare no conflicts of interest.

678

679 ## 7.3. Funding information

680 This research was funded in part by the Wellcome Trust (103740/Z/14/Z and
681 108905/B/15/Z) and through support from the 'Supporting Evidence Based
682 Interventions' and Bill and Melinda Gates foundation, and a Royal Society GCRF
683 Challenge grant CH160034, both awarded to KM. For the purpose of open access,
684 the author has applied a CC BY public copyright licence to any Author Accepted
685 Manuscript version arising from this submission.

686

687 KM was supported by a Wellcome Trust Investigator award grant (103740/Z/14/Z),
688 GO by a Wellcome Trust PhD studentship (108905/B/15/Z), and JLP by a Royal
689 Society GCRF Challenge grant CH160034.

690

691 ## 7.4. Ethical approval

692 Not applicable.

693

694 ## 7.5. Consent for publication

695 Not applicable.

696

697 ## 7.6. Acknowledgments

698

699 We thank Steven Kelly (University of Oxford) for his comments and insights on the
700 manuscript.

8. Supplementary material

(a)

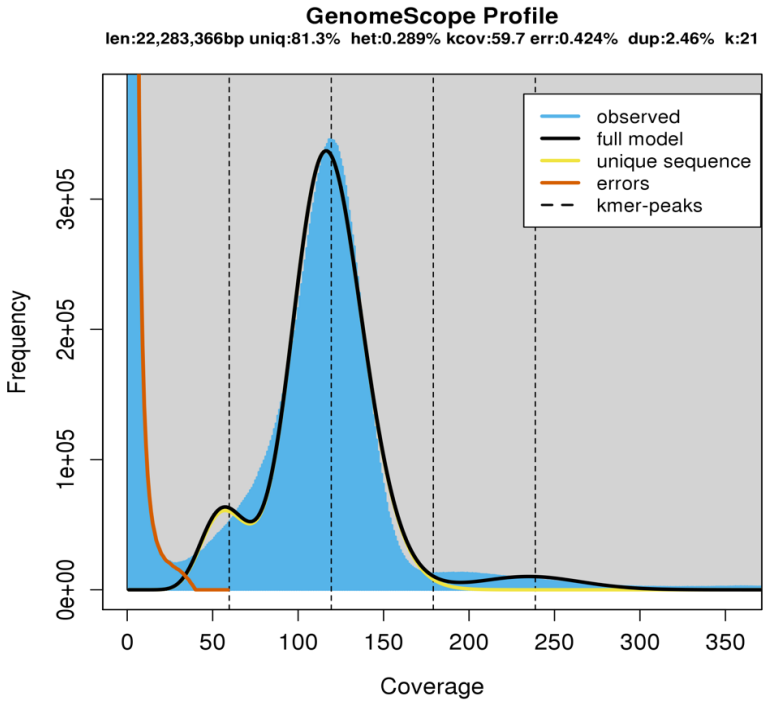

(b)

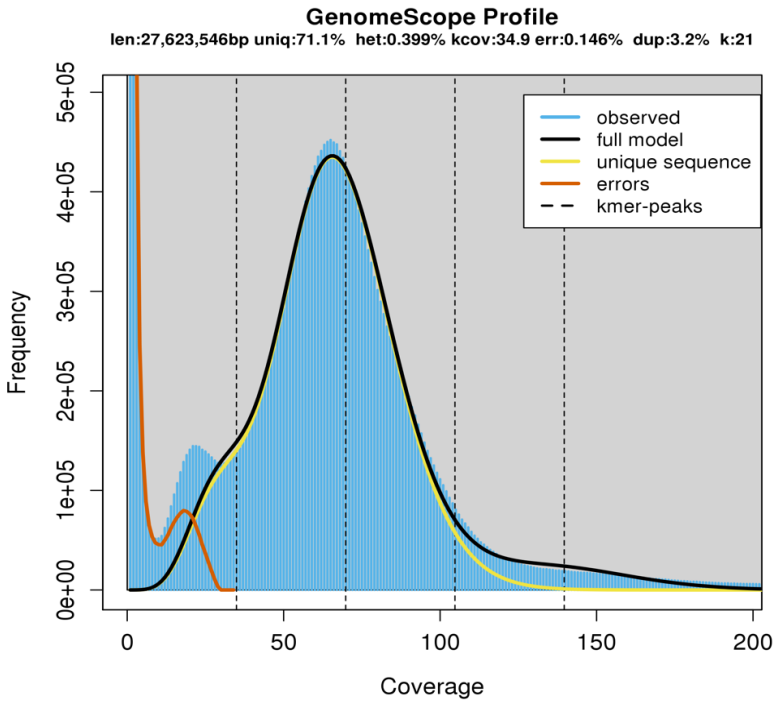

Supplementary Figure S1: k-mer spectra of (a) *T. melophagium* and (b) *T. theileri* using a k-mer size of 21. The statistics presented in these images represent the lowest estimate size, the highest estimate was used in Table 1 as these had a greater model fit.

(a)

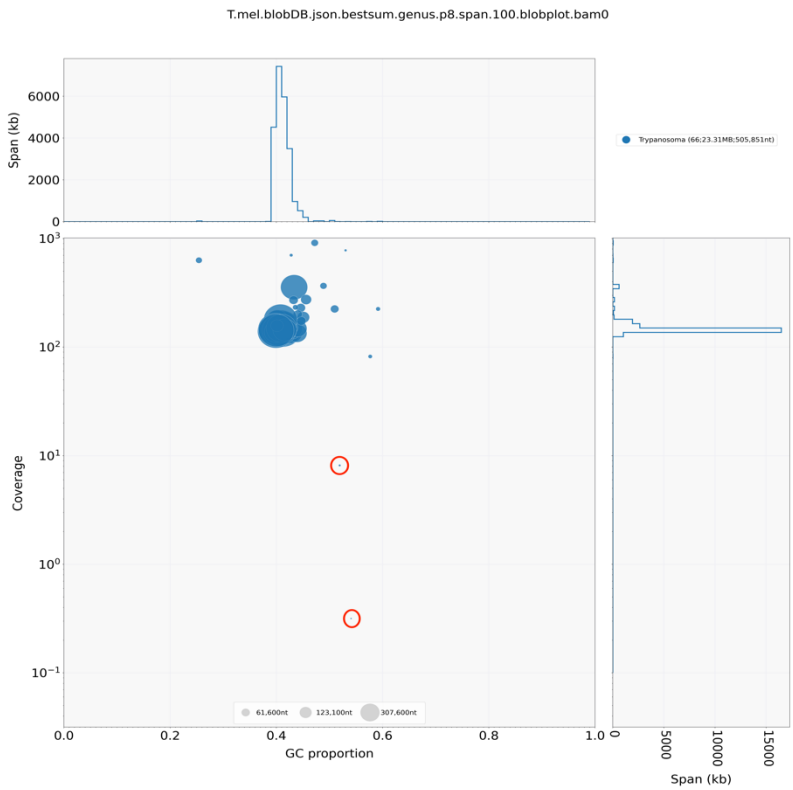

(b)

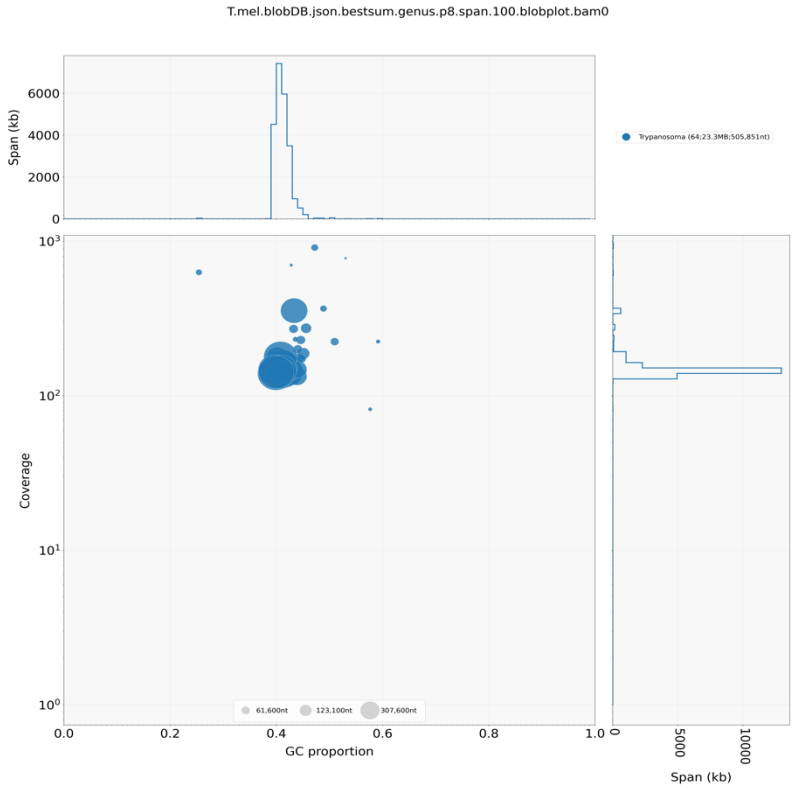

Supplementary Figure S2: Coverage and blast annotation for (a) the polished assembly and (b) the manually trimmed assembly.

(a)

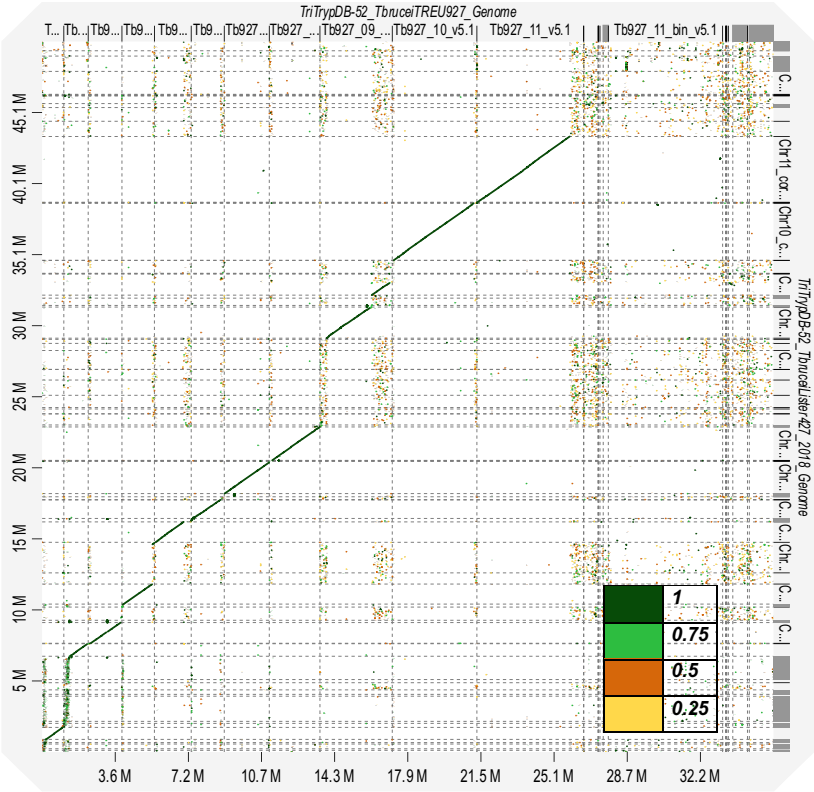

(b)

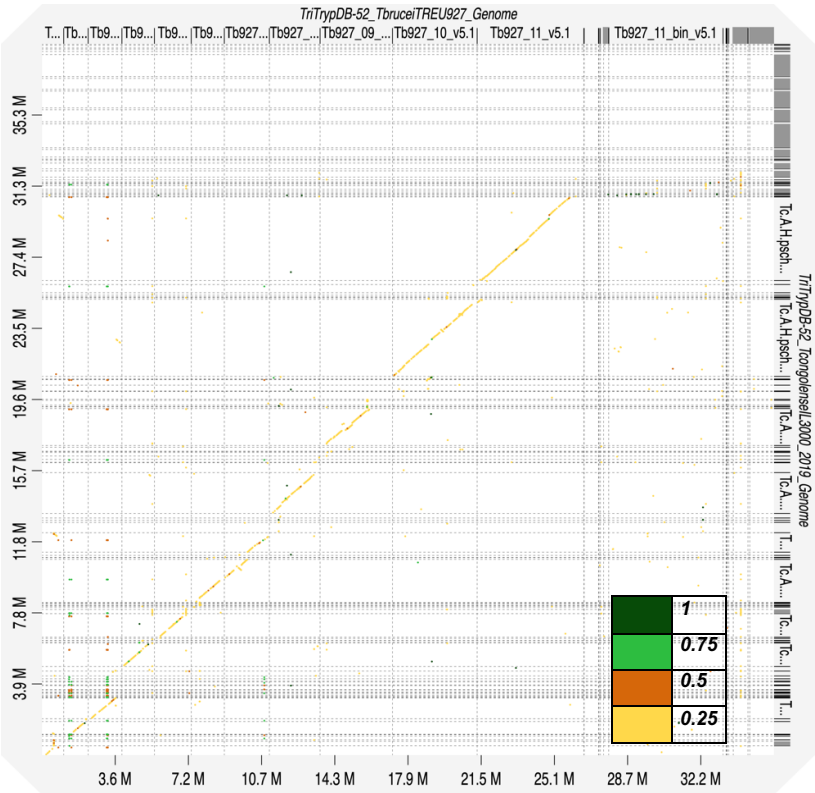

Supplementary Figure S3: Synteny plot of (a) *T. brucei* TREU927/4 and *T. brucei* Lister 427 and (b) *T. brucei* TREU927/4 *and T. congolense* IL3000 2019 genome sequences. The legend refers to the identity between the sequences.

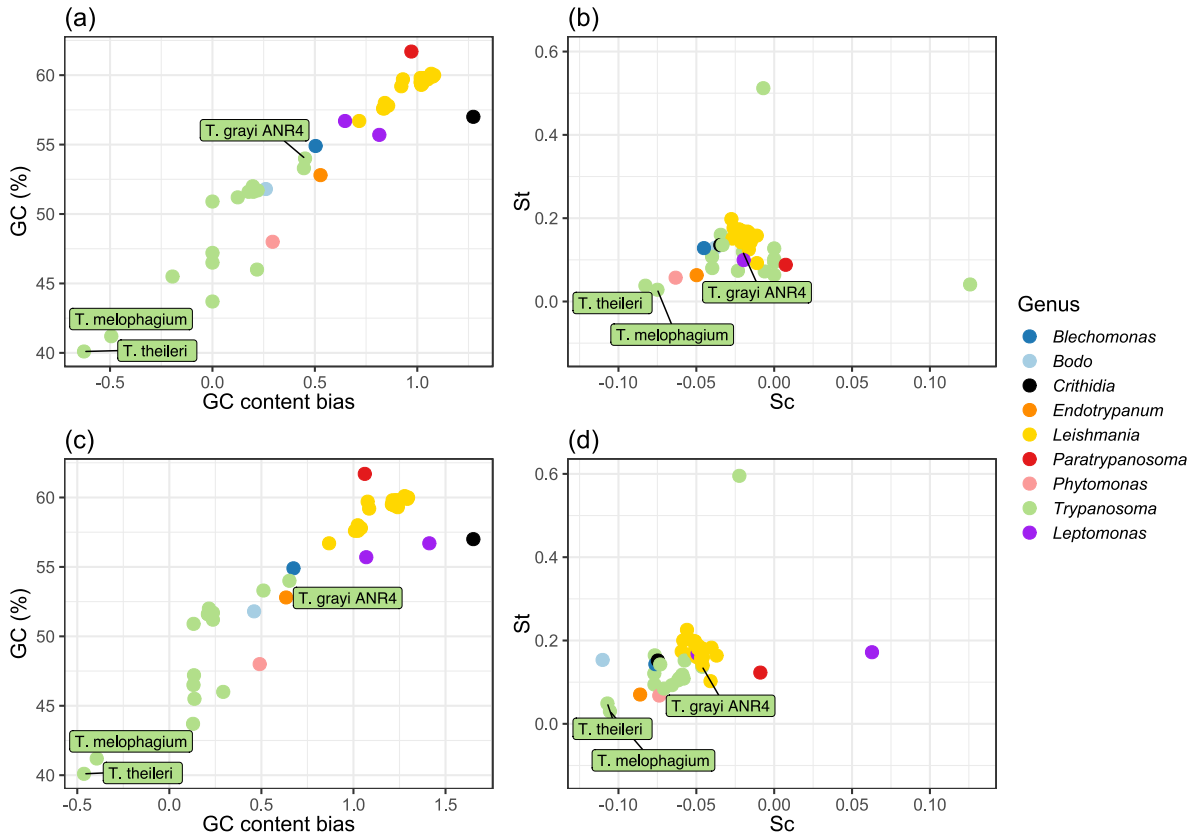

775

776 **Supplementary Figure S4:** (a) GC content across the whole genome and GC

777 content bias in a every CDS. (b) Selection acting on translational efficiency (St) and

778 selection acting on nucleotide cost (Sc). (c) GC content across the whole genome

779 and GC content bias in CDS of a trypanosomatid universal single copy orthologue

780 which is essential in every life cycle stage in *T. brucei* (n=158). (d) Selection acting

781 on translational efficiency (St) and selection acting on nucleotide cost (Sc) in

782 trypanosomatid universal single copy orthologues which is essential in every life

783 cycle stage in *T. brucei* (n=158).

784 **Table S1:** Software, including the version and any options used.

Tool	Version	Flag	Available at
Guppy	4.0.15	--flowcell FLO-MIN106 --kit SQK-RAD004	https://community.nanoporetech.com/
Trimmomatic	0.39	SLIDINGWINDOW 4:20 MINLEN 50	https://github.com/timflutre/trimmomatic
GenomeScope	1	Kmer 21 Max kmer cov. 1000	http://qb.cshl.edu/genomescope/
Jellyfish	2.2.10	-C -m 21 -s 1000000000	https://github.com/gmarcais/Jellyfish
Wtdbg2	3	-x ont -g 30m -A -t 10	https://github.com/ruanjue/wtdbg2
Minimap2	2.17-r941	-ax map-ont	https://github.com/lh3/minimap2
Racon	v1.4.13	-m 8 -x -6 -g -8 -w 500	https://github.com/isovic/racon
Medaka	V5	-m r941_min_high_g360	https://github.com/nanoporetech/medaka
BWA-MEM	0.7.17-r1188	N/A	https://github.com/lh3/bwa
Pilon	1.24	--genome --diploid –bam	https://github.com/broadinstitute/pilon

		--bam	
Blast	2.6.0+	blastn -task megablast -outfmt '6 qseqid staxids bitscore std' -max_target_seqs 1 -max_hsps 1 -evalue 1e-25 or 1e-5	ftp://ftp.ncbi.nlm.nih.gov/blast/executables/blast+/LATEST/
DIAMOND	2.0.5.143	Blastx --sensitive --max-target-seqs 1 --evalue 1e-25	http://www.diamondsearch.org
BlobTools	1.1.1	-r genus	https://github.com/DRL/blobtools
Scaffold_stats	N/A	N/A	https://github.com/sujaikumar/assemblage
BUSCO	V5	-l euglenozoa_odb10	https://busco.ezlab.org/
RepeatModeler	N/A	-database -LTRStruct -pa 8	http://www.repeatmasker.org/RepeatModeler/
RepeatMasker	N/A	-lib consensi.fa.classified -pa 8 -xsmall -nolow –gff	http://www.repeatmasker.org/RMDownload.html

BRAKER2	2.1.6	--prot_seq --bam --softmasking --etpmode --gff3	https://github.com/Gaius-Augustus/BRAKER
D-Genies	1.2.0	-Minimap2	http://dgenies.toulouse.inra.fr/run
tRNAscan-SE	2.0.9	-E	http://lowelab.ucsc.edu/tRNAscan-SE/
CodonMuse	0.1.0	-f -tscan	https://github.com/easeward/CodonMuSe
OrthoFinder	2.5.2	-S diamond_ultra_sens	https://github.com/davidemms/OrthoFinder
InterProScan	5.52-86.0	--dp --goterms -appl SignalP-EUK-4.1, Pfam -f TSV	https://www.ebi.ac.uk/interpro/
KinFin	1.0.3		https://github.com/DRL/kinfin
R	3.6.1		https://www.r-project.org/
ggplot2	3.3.3		https://cran.r-project.org/web/packages/ggplot2/index.html

ggrepel	0.9.1		https://cran.r-project.org/web/packages/ggrepel/index.html
dplyr	1.0.5		https://cran.r-project.org/web/packages/dplyr/index.html

787 ## 9. References

788 1. Podlipaev S. The more insect trypanosomatids under study-the more diverse
789 Trypanosomatidae appears. Int J Parasitol. 2001;31(5-6):648-52.
790 2. Kaufer A, Ellis J, Stark D, Barratt J. The evolution of trypanosomatid
791 taxonomy. Parasit Vectors. 2017;10(1):287.
792 3. Schnaufer A, Domingo GJ, Stuart K. Natural and induced dyskinetoplastic
793 trypanosomatids: how to live without mitochondrial DNA. International Journal for
794 Parasitology. 2002;32(9):1071-84.
795 4. Cayla M, Rojas F, Silvester E, Venter F, Matthews KR. African trypanosomes.
796 Parasit Vectors. 2019;12(1):190.
797 5. Mehlitz D, Molyneux DH. The elimination of Trypanosoma brucei gambiense?
798 Challenges of reservoir hosts and transmission cycles: Expect the unexpected.
799 Parasite Epidemiol Control. 2019;6:e00113.
800 6. Cavalier-Smith T. Kingdoms Protozoa and Chromista and the eozoan root of
801 the eukaryotic tree. Biol Lett. 2010;6(3):342-5.
802 7. Burki F. The eukaryotic tree of life from a global phylogenomic perspective.
803 Cold Spring Harb Perspect Biol. 2014;6(5):a016147.
804 8. Maslov DA, Opperdoes FR, Kostygov AY, Hashimi H, Lukes J, Yurchenko V.
805 Recent advances in trypanosomatid research: genome organization, expression,
806 metabolism, taxonomy and evolution. Parasitology. 2019;146(1):1-27.
807 9. Melville SE, Leech V, Gerrard CS, Tait A, Blackwell JM. The molecular
808 karyotype of the megabase chromosomes of Trypanosoma brucei and the
809 assignment of chromosome markers. Mol Biochem Parasitol. 1998;94(2):155-73.

810 10. Wickstead B, Ersfeld K, Gull K. The small chromosomes of Trypanosoma
811 brucei involved in antigenic variation are constructed around repetitive palindromes.
812 Genome Res. 2004;14(6):1014-24.
813 11. Daniels JP, Gull K, Wickstead B. Cell biology of the trypanosome genome.
814 Microbiol Mol Biol Rev. 2010;74(4):552-69.
815 12. Parsons M, Nelson RG, Watkins KP, Agabian N. Trypanosome mRNAs share
816 a common 5' spliced leader sequence. Cell. 1984;38(1):309-16.
817 13. Clayton C. Regulation of gene expression in trypanosomatids: living with
818 polycistronic transcription. Open Biol. 2019;9(6):190072.
819 14. Steinert M. Mitochondria Associated with the Kinetonucleus of Trypanosoma
820 Mega. J Biophys Biochem Cytol. 1960;8(2):542-6.
821 15. Kleisen CMaBP. Sequence heterogeneity of the mini-circles of kinetoplast
822 DNA of Crithidia luciliae and evidence for the presence of a component more
823 complex than mini-circle DNA in the kinetoplast network. Biochimica et Biophysica
824 Acta (BBA) - Nucleic Acids and Protein Synthesis. 1975;407(4):473-8.
825 16. Borst P, Fase-Fowler F. The maxi-circle of Trypanosoma brucei kinetoplast
826 DNA. Biochim Biophys Acta. 1979;565(1):1-12.
827 17. Simpson L. Isolation of maxicircle component of kinetoplast DNA from
828 hemoflagellate protozoa. Proc Natl Acad Sci U S A. 1979;76(4):1585-8.
829 18. Berriman M, Ghedin E, Hertz-Fowler C, Blandin G, Renauld H, Bartholomeu
830 DC, *et al*. The genome of the African trypanosome Trypanosoma brucei. Science.
831 2005;309(5733):416-22.
832 19. Borst P. Antigenic variation and allelic exclusion. Cell. 2002;109(1):5-8.
833 20. Pays E, Vanhamme L, Perez-Morga D. Antigenic variation in Trypanosoma
834 brucei: facts, challenges and mysteries. Curr Opin Microbiol. 2004;7(4):369-74.

835 21. Buscaglia CA, Campo VA, Frasch AC, Di Noia JM. Trypanosoma cruzi
836 surface mucins: host-dependent coat diversity. Nat Rev Microbiol. 2006;4(3):229-36.
837 22. Nardy AF, Freire-de-Lima CG, Perez AR, Morrot A. Role of Trypanosoma
838 cruzi Trans-sialidase on the Escape from Host Immune Surveillance. Front Microbiol.
839 2016;7:348.
840 23. Yao C, Donelson JE, Wilson ME. The major surface protease (MSP or GP63)
841 of Leishmania sp. Biosynthesis, regulation of expression, and function. Mol Biochem
842 Parasitol. 2003;132(1):1-16.
843 24. Funk S, Nishiura H, Heesterbeek H, Edmunds WJ, Checchi F. Identifying
844 Transmission Cycles at the Human-Animal Interface: The Role of Animal Reservoirs
845 in Maintaining Gambiense Human African Trypanosomiasis. Plos Computational
846 Biology. 2013;9(1):e1002855.
847 25. Matthews DM, Kingston N, Maki L, Nelms G. Trypanosoma theileri Laveran,
848 1902, in Wyoming cattle. Am J Vet Res. 1979;40(5):623-9.
849 26. Schlafer DH. Trypanosoma theileri: a literature review and report of incidence
850 in New York cattle. Cornell Vet. 1979;69(4):411-25.
851 27. Farrar RG, Klei TR. Prevalence of Trypanosoma theileri in Louisiana cattle. J
852 Parasitol. 1990;76(5):734-6.
853 28. Mott GA, Wilson R, Fernando A, Robinson A, MacGregor P, Kennedy D, *et al*.
854 Targeting Cattle-Borne Zoonoses and Cattle Pathogens Using a Novel
855 Trypanosomatid-Based Delivery System. Plos Pathogens. 2011;7(10):e1002340.
856 29. Bose R, Heister NC. Development of Trypanosoma (M.) theileri in tabanids. J
857 Eukaryot Microbiol. 1993;40(6):788-92.

858 30. Doherty ML, Windle H, Voorheis HP, Larkin H, Casey M, Clery D, *et al*.
859 Clinical disease associated with Trypanosoma theileri infection in a calf in Ireland.
860 Vet Rec. 1993;132(26):653-6.
861 31. Seifi HA. Clinical Trypanosomosis Due to Trypanosoma-Theileri in a Cow in
862 Iran. Tropical Animal Health and Production. 1995;27(2):93-4.
863 32. Kelly S, Ivens A, Mott GA, O'Neill E, Emms D, Macleod O, *et al*. An
864 Alternative Strategy for Trypanosome Survival in the Mammalian Bloodstream
865 Revealed through Genome and Transcriptome Analysis of the Ubiquitous Bovine
866 Parasite Trypanosoma (Megatrypanum) theileri. Genome Biology and Evolution.
867 2017;9(8):2093-109.
868 33. Gibson W, Pilkington JG, Pemberton JM. Trypanosoma melophagium from
869 the sheep ked Melophagus ovinus on the island of St Kilda. Parasitology.
870 2010;137(12):1799-804.
871 34. Martinkovic F, Matanovic K, Rodrigues AC, Garcia HA, Teixeira MM.
872 Trypanosoma (Megatrypanum) melophagium in the sheep ked Melophagus ovinus
873 from organic farms in Croatia: phylogenetic inferences support restriction to sheep
874 and sheep keds and close relationship with trypanosomes from other ruminant
875 species. J Eukaryot Microbiol. 2012;59(2):134-44.
876 35. Serpil. Trypanosoma melophagium in blood cell culture. Ankara Üniversitesi
877 Veteriner Fakültesi Dergisi. 2008;50(1):1-.
878 36. Flu. Über die Flagellaten im Darm von Melophagus ovinus. Arch. f.
879 37. Porter A. The Structure and Life-history of Crithidia melophagia (Flu), an
880 Endoparasite of the Sheep Ked, Melophagus ovinus.

881 38. Swingle LD. The Relation of Crithidia melophagia to the Sheep's Blood, with
882 Remarks upon the Controversy between Dr. Porter and Dr. Woodcock. Transactions
883 of the American Microscopical Society. 1911;30(4):275.
884 39. Hoare CA. An Experimental Study of the Sheep-Trypanosome (T.
885 melophagium Flu, 1908), and its Transmission by the Sheep-Ked (Melophagus
886 ovinus L.). Parasitology. 1923;15(4):365-424.
887 40. Hoare CA. The trypanosomes of mammals. A zoological monograph. The
888 trypanosomes of mammals A zoological monograph , sciwheel-projects =
889 Monomorphism. 1972.
890 41. Underwood WJaBRaDMLaGRaMSAaSA. Biology and diseases of ruminants
891 (sheep, goats, and cattle). Laboratory Animal Medicine: Elsevier; 2015. p. 623-94.
892 42. Chainey JE. Horse-flies, deer-flies and clegs (Tabanidae). In: Lane RPaCRW,
893 editor. Medical insects and arachnids. Dordrecht , sciwheel-projects = T-mel vs T-
894 the: Springer Netherlands; 1993. p. 310-32.
895 43. Leger AaLT. pycoQC , interactive quality control for Oxford Nanopore
896 Sequencing. The Journal of Open Source Software. 2019;4(34):1236.
897 44. Bolger AM, Lohse M, Usadel B. Trimmomatic: a flexible trimmer for Illumina
898 sequence data. Bioinformatics. 2014;30(15):2114-20.
899 45. Marcais G, Kingsford C. A fast, lock-free approach for efficient parallel
900 counting of occurrences of k-mers. Bioinformatics. 2011;27(6):764-70.
901 46. Vurture GW, Sedlazeck FJ, Nattestad M, Underwood CJ, Fang H, Gurtowski
902 J, *et al*. GenomeScope: fast reference-free genome profiling from short reads.
903 Bioinformatics. 2017;33(14):2202-4.
904 47. Ruan J, Li H. Fast and accurate long-read assembly with wtdbg2. Nat
905 Methods. 2020;17(2):155-8.

906 48. Li H. Aligning sequence reads, clone sequences and assembly contigs with
907 BWA - MEM. arXiv , sciwheel-projects = Software. 2013.
908 49. Li H. Minimap2: pairwise alignment for nucleotide sequences. Bioinformatics.
909 2018;34(18):3094-100.
910 50. Vaser R, Sovic I, Nagarajan N, Sikic M. Fast and accurate de novo genome
911 assembly from long uncorrected reads. Genome Res. 2017;27(5):737-46.
912 51. Walker BJ, Abeel T, Shea T, Priest M, Abouelliel A, Sakthikumar S, *et al*.
913 Pilon: an integrated tool for comprehensive microbial variant detection and genome
914 assembly improvement. PLoS One. 2014;9(11):e112963.
915 52. Seppey M, Manni M, Zdobnov EM. BUSCO: Assessing Genome Assembly
916 and Annotation Completeness. Methods Mol Biol. 2019;1962:227-45.
917 53. Buchfink B, Xie C, Huson DH. Fast and sensitive protein alignment using
918 DIAMOND. Nature Methods. 2015;12(1):59-60.
919 54. Jones P, Binns D, Chang HY, Fraser M, Li W, McAnulla C, *et al*. InterProScan
920 5: genome-scale protein function classification. Bioinformatics. 2014;30(9):1236-40.
921 55. Laetsch DRaBML. BlobTools : Interrogation of genome assemblies.
922 F1000Research. 2017;6:1287.
923 56. Flynn JM, Hubley R, Goubert C, Rosen J, Clark AG, Feschotte C, *et al*.
924 RepeatModeler2 for automated genomic discovery of transposable element families.
925 Proc Natl Acad Sci U S A. 2020;117(17):9451-7.
926 57. Kriventseva EV, Kuznetsov D, Tegenfeldt F, Manni M, Dias R, Simao FA, *et*
927 *al*. OrthoDB v10: sampling the diversity of animal, plant, fungal, protist, bacterial and
928 viral genomes for evolutionary and functional annotations of orthologs. Nucleic Acids
929 Res. 2019;47(D1):D807-D11.

930 58. Hoff KJ, Lange S, Lomsadze A, Borodovsky M, Stanke M. BRAKER1:
931 Unsupervised RNA-Seq-Based Genome Annotation with GeneMark-ET and
932 AUGUSTUS. Bioinformatics. 2016;32(5):767-9.
933 59. Stanke M, Schoffmann O, Morgenstern B, Waack S. Gene prediction in
934 eukaryotes with a generalized hidden Markov model that uses hints from external
935 sources. Bmc Bioinformatics. 2006;7:62.
936 60. Gotoh O. A space-efficient and accurate method for mapping and aligning
937 cDNA sequences onto genomic sequence. Nucleic Acids Res. 2008;36(8):2630-8.
938 61. Stanke M, Diekhans M, Baertsch R, Haussler D. Using native and syntenically
939 mapped cDNA alignments to improve de novo gene finding. Bioinformatics.
940 2008;24(5):637-44.
941 62. Li H, Handsaker B, Wysoker A, Fennell T, Ruan J, Homer N, *et al*. The
942 Sequence Alignment/Map format and SAMtools. Bioinformatics. 2009;25(16):2078-9.
943 63. Barnett DW, Garrison EK, Quinlan AR, Stromberg MP, Marth GT. BamTools:
944 a C++ API and toolkit for analyzing and managing BAM files. Bioinformatics.
945 2011;27(12):1691-2.
946 64. Iwata H, Gotoh O. Benchmarking spliced alignment programs including
947 Spaln2, an extended version of Spaln that incorporates additional species-specific
948 features. Nucleic Acids Research. 2012;40(20):e161.
949 65. Lomsadze A, Burns PD, Borodovsky M. Integration of mapped RNA-Seq
950 reads into automatic training of eukaryotic gene finding algorithm. Nucleic Acids
951 Research. 2014;42(15):e119.
952 66. Hoff KJ, Lomsadze A, Borodovsky M, Stanke M. Whole-Genome Annotation
953 with BRAKER. Methods Mol Biol. 2019;1962:65-95.

954 67. Bruna T, Lomsadze A, Borodovsky M. GeneMark-EP+: eukaryotic gene
955 prediction with self-training in the space of genes and proteins. NAR Genom
956 Bioinform. 2020;2(2):lqaa026.
957 68. Bruna T, Hoff KJ, Lomsadze A, Stanke M, Borodovsky M. BRAKER2:
958 automatic eukaryotic genome annotation with GeneMark-EP+ and AUGUSTUS
959 supported by a protein database. NAR Genom Bioinform. 2021;3(1):lqaa108.
960 69. Nielsen H. Predicting Secretory Proteins with SignalP. Methods Mol Biol.
961 2017;1611:59-73.
962 70. Mistry J, Chuguransky S, Williams L, Qureshi M, Salazar GA, Sonnhammer
963 ELL, *et al*. Pfam: The protein families database in 2021. Nucleic Acids Res.
964 2021;49(D1):D412-D9.
965 71. Cabanettes F, Klopp C. D-GENIES: dot plot large genomes in an interactive,
966 efficient and simple way. PeerJ. 2018;6:e4958.
967 72. Aslett M, Aurrecoechea C, Berriman M, Brestelli J, Brunk BP, Carrington M, *et*
968 *al*. TriTrypDB: a functional genomic resource for the Trypanosomatidae. Nucleic
969 Acids Research. 2010;38:D457-D62.
970 73. Leinonen R, Sugawara H, Shumway M, International Nucleotide Sequence
971 Database C. The sequence read archive. Nucleic Acids Res. 2011;39(Database
972 issue):D19-21.
973 74. Chan PP, Lin BY, Mak AJ, Lowe TM. tRNAscan-SE 2.0: improved detection
974 and functional classification of transfer RNA genes. Nucleic Acids Research.
975 2021;49(16):9077-96.
976 75. Seward EA, Kelly S. Selection-driven cost-efficiency optimization of
977 transcripts modulates gene evolutionary rate in bacteria. Genome Biology. 2018;19.

978 76. Seward EA, Kelly S. Dietary nitrogen alters codon bias and genome
979 composition in parasitic microorganisms. Genome Biology. 2016;17.
980 77. Alsford S, Turner DJ, Obado SO, Sanchez-Flores A, Glover L, Berriman M, *et*
981 *al*. High-throughput phenotyping using parallel sequencing of RNA interference
982 targets in the African trypanosome. Genome Research. 2011;21(6):915-24.
983 78. Emms DM, Kelly S. OrthoFinder: phylogenetic orthology inference for
984 comparative genomics. Genome Biol. 2019;20(1):238.
985 79. Laetsch DR, Blaxter ML. KinFin: Software for Taxon-Aware Analysis of
986 Clustered Protein Sequences. G3 (Bethesda). 2017;7(10):3349-57.
987 80. Emms DM, Kelly S. STRIDE: Species Tree Root Inference from Gene
988 Duplication Events. Mol Biol Evol. 2017;34(12):3267-78.
989 81. Emms DaKS. STAG : Species Tree Inference from All Genes. BioRxiv. 2018.
990 82. Letunic I, Bork P. Interactive Tree Of Life (iTOL): an online tool for
991 phylogenetic tree display and annotation. Bioinformatics. 2007;23(1):127-8.
992 83. Team RC. R: A Language and Environment for Statistical Computing. R
993 Foundation for Statistical Computing; 2019.
994 84. Wickham H. ggplot2: elegant graphics for data analysis. 2016.
995 85. Slowikowski K. ggrepel: Automatically Position Non-Overlapping Text Labels
996 with'ggplot2'. R package version 08 0 ed. 2018.
997 86. Oldrieve G, Verney M, Jaron KS, Hebert L, Matthews KR. Monomorphic
998 Trypanozoon: towards reconciling phylogeny and pathologies. Microb Genom.
999 2021;7(8).
1000 87. Kniepert FW. Blood-feeding and nectar-feeding in adult tabanidae (Diptera).
1001 Oecologia. 1980;46(1):125-9.

1002 88. Sanchez-Moreno M, Lasztity D, Coppens I, Opperdoes FR. Characterization
1003 of carbohydrate metabolism and demonstration of glycosomes in a Phytomonas sp.
1004 isolated from Euphorbia characias. Mol Biochem Parasitol. 1992;54(2):185-99.
1005 89. Jaskowska E, Butler C, Preston G, Kelly S. Phytomonas: trypanosomatids
1006 adapted to plant environments. PLoS Pathog. 2015;11(1):e1004484.
1007 90. Mony BM, MacGregor P, Ivens A, Rojas F, Cowton A, Young J, *et al*.
1008 Genome-wide dissection of the quorum sensing signalling pathway in Trypanosoma
1009 brucei. Nature. 2014;505(7485):681-5.
1010 91. Cayla M, McDonald L, MacGregor P, Matthews K. An atypical DYRK kinase
1011 connects quorum-sensing with posttranscriptional gene regulation in Trypanosoma
1012 brucei. Elife. 2020;9.
1013 92. Ling AS, Trotter JR, Hendriks EF. A zinc finger protein, TbZC3H20, stabilizes
1014 two developmentally regulated mRNAs in trypanosomes. J Biol Chem.
1015 2011;286(23):20152-62.
1016 93. Liu B, Kamanyi Marucha K, Clayton C. The zinc finger proteins ZC3H20 and
1017 ZC3H21 stabilise mRNAs encoding membrane proteins and mitochondrial proteins
1018 in insect-form Trypanosoma brucei. Mol Microbiol. 2020;113(2):430-51.
1019 94. Toh JY, Nkouawa A, Sanchez SR, Shi H, Kolev NG, Tschudi C. Identification
1020 of positive and negative regulators in the stepwise developmental progression
1021 towards infectivity in Trypanosoma brucei. Sci Rep. 2021;11(1):5755.
1022 95. Szoor B, Ruberto I, Burchmore R, Matthews KR. A novel phosphatase
1023 cascade regulates differentiation in Trypanosoma brucei via a glycosomal signaling
1024 pathway. Genes Dev. 2010;24(12):1306-16.

1025 96. Domingo-Sananes MR, Szoor B, Ferguson MA, Urbaniak MD, Matthews KR.
1026 Molecular control of irreversible bistability during trypanosome developmental
1027 commitment. J Cell Biol. 2015;211(2):455-68.
1028 97. Szoor B, Wilson J, McElhinney H, Tabernero L, Matthews KR. Protein
1029 tyrosine phosphatase TbPTP1: A molecular switch controlling life cycle differentiation
1030 in trypanosomes. J Cell Biol. 2006;175(2):293-303.
1031 98. Walrad P, Paterou A, Acosta-Serrano A, Matthews KR. Differential
1032 trypanosome surface coat regulation by a CCCH protein that co-associates with
1033 procyclin mRNA cis-elements. PLoS Pathog. 2009;5(2):e1000317.
1034 99. Gale M, Jr., Parsons M. A Trypanosoma brucei gene family encoding protein
1035 kinases with catalytic domains structurally related to Nek1 and NIMA. Mol Biochem
1036 Parasitol. 1993;59(1):111-21.
1037 100. Gale M, Jr., Carter V, Parsons M. Translational control mediates the
1038 developmental regulation of the Trypanosoma brucei Nrk protein kinase. J Biol
1039 Chem. 1994;269(50):31659-65.
1040 101. Jones NG, Thomas EB, Brown E, Dickens NJ, Hammarton TC, Mottram JC.
1041 Regulators of Trypanosoma brucei cell cycle progression and differentiation
1042 identified using a kinome-wide RNAi screen. PLoS Pathog. 2014;10(1):e1003886.
1043 102. Muller IB, Domenicali-Pfister D, Roditi I, Vassella E. Stage-specific
1044 requirement of a mitogen-activated protein kinase by Trypanosoma brucei. Mol Biol
1045 Cell. 2002;13(11):3787-99.
1046 103. Mony BM, Matthews KR. Assembling the components of the quorum sensing
1047 pathway in African trypanosomes. Mol Microbiol. 2015;96(2):220-32.
1048 104. Pool JE, Nielsen R. Population size changes reshape genomic patterns of
1049 diversity. Evolution. 2007;61(12):3001-6.

1050 105. Cooper D, Eleftherianos I. Memory and Specificity in the Insect Immune
1051 System: Current Perspectives and Future Challenges. Front Immunol. 2017;8:539.
1052 106. Wang F, Ekiert DC, Ahmad I, Yu W, Zhang Y, Bazirgan O, *et al*. Reshaping
1053 antibody diversity. Cell. 2013;153(6):1379-93.
1054 107. Emms DM, Kelly S. Benchmarking Orthogroup Inference Accuracy: Revisiting
1055 Orthobench. Genome Biology and Evolution. 2020;12(12):2258-66.
1056 108. Ullu E, Tschudi C, Chakraborty T. RNA interference in protozoan parasites.
1057 Cellular Microbiology. 2004;6(6):509-19.
1058